Werk

Jahr: 1985
Kollektion: fid.geo
Signatur: 8 Z NAT 2148:57
Digitalisiert: Niedersächsische Staats- und Universitätsbibliothek Göttingen
Werk Id: PPN1015067948_0057
PURL: http://resolver.sub.uni-goettingen.de/purl?PPN1015067948_0057

LOG Id: LOG_0027
LOG Titel: First results and preliminary interpretation of deep-reflection seismic recordings along profile DEKORP 2-South
LOG Typ: article

Übergeordnetes Werk

Werk Id: PPN1015067948
PURL: http://resolver.sub.uni-goettingen.de/purl?PPN1015067948
OPAC: http://opac.sub.uni-goettingen.de/DB=1/PPN?PPN=1015067948

Contact

Niedersächsische Staats- und Universitätsbibliothek Göttingen
Georg-August-Universität Göttingen
Platz der Göttinger Sieben 1
37073 Göttingen
Germany
Email: gdz@sub.uni-goettingen.de

J Geophys (1985) 57:137–163

Journal of Geophysics

First results and preliminary interpretation of deep-reflection seismic recordings along profile DEKORP 2-South

DEKORP Research Group

Contributors: **R.K. Bortfeld, J. Gowin, M. Stiller** (Institut für Geophysik, Arnold-Sommerfeld-Str. 1, 3392 Clausthal-Zellerfeld); **B. Baier** (Institut für Geophysik, Feldbergstr. 47, 6000 Frankfurt/M.); **H.J. Behr, T. Heinrichs** (Institut für Geologie und Dynamik der Lithosphäre, Goldschmidtstr. 3, 3400 Göttingen); **H.J. Dürbaum, A. Hahn, C. Reichert, J. Schmoll** (Bundesanstalt für Geowissenschaften und Rohstoffe/ Niedersächsisches Landesamt für Bodenforschung, Stilleweg 2, 3000 Hannover 51); **G. Dohr** (Preussag AG, Arndtstr. 1, 3000 Hannover 1); **R. Meissner, R. Bittner, B. Milkereit** (Institut für Geophysik, Olshausenstr. 40–60, 2300 Kiel 1); **H. Gebrande** (Institut für Allgemeine und Angewandte Geophysik, Theresienstr. 41/IV, 8000 München 2)

Abstract. In 1984 the DEKORP reflection seismic crustal studies have been started on a large scale in the Federal Republic of Germany as a contribution to the International Lithosphere Project, the European Geotraverse and the German Deep Drilling Program. The first 250 km long profile DEKORP 2-South has been observed between the Nördlinger Ries and the Taunus crossing the boundaries between the Variscan belt units Moldanubian, Saxothuringian and Rhenohercynian. This paper gives an overview of the measurements and data processing. From the steep-angle observations on the main profile a seismic section was prepared which is dominated by diffraction events. These events are analyzed with respect to velocities and structural information. Also wide-angle observations on the main profile and on a parallel profile have been carried out. A geological/geophysical interpretation of the near-vertical reflection data has been attempted and is presented in this paper: there are strong indications of large-scale horizontal tectonics affecting the upper and lower crust down to the Moho depth of 26–29 km.

Key words: Deep reflection seismic profiling – DEKORP – Mid-European Variscides – Crustal structure – Diffraction clusters – Ductile shear tectonics – Intracrustal thrust system – Mid German Crystalline High

1. Introduction and concept of DEKORP

1.1 Overview

DEKORP = *De*utsches *ko*ntinentales *r*eflexionsseismisches *P*rogramm (German continental reflection seismic program) was initiated and planned by a group of earth scientists from the Federal Republic of Germany in 1982. It is tightly connected to the German contribution to the International Lithosphere Program, especially to the German Deep Drilling Program (KTB = *K*ontinentales *T*ief*b*ohrprogramm) (Althaus et al., 1984) and the *E*uropean *Geo*traverse (EGT) (Giese, 1983). DEKORP has been conceived as a network of vertical reflection seismic traverses crossing the major geotectonic units in roughly strike and dip direction and thus contributing to the German part of the EGT study area.

The main objectives of DEKORP are:
– A detailed investigation of the Earth's crust in Germany by seismic reflection measurements along seismic profiles of great length.
– A combination of the reflection measurements with other geophysical and geological studies in order to reveal the tectonic structure and development of the Variscan orogenesis.

In the northern part of Germany, in the Upper Rhine Valley and in the Alpine Molasse Basin many seismic reflection lines have been observed in the last 40 years mostly in prospecting for hydrocarbons, some of them collecting additional valuable information down to more than 30 km (Dohr, 1957a; Dohr, 1957b; Bally, 1983). In the Variscan area, i.e. the German Mittelgebirge, abundant seismic refraction profiles exist (Giese et al., 1976). Also some short special crustal reflection profiles have been observed in this area in the last 20 years (Angenheister and Pohl, 1969; Dohr and Meissner, 1975; Bartelsen et al., 1982; Meissner et al., 1982, 1983). The planned profile network of DEKORP with its long lines should provide a regional overview of the crustal structure, define the various tectonic boundaries and combine the information from the north with those in the southern part. The DEKORP network is shown in Fig. 1 together with some of the previously observed shorter reflection profiles and some general geological information. The DEKORP profiles are arranged about parallel and perpendicular to the strike direction of the Variscan mountains. They have a typical length of several hundreds of kilometers. A close cooperation between industry and research institutes is considered an essential requirement.

The following gives a rough idea of the structure of DEKORP's organization: All important decisions are taken by DEKORP's steering committee consisting of

Offprint requests to: H.-J. Dürbaum

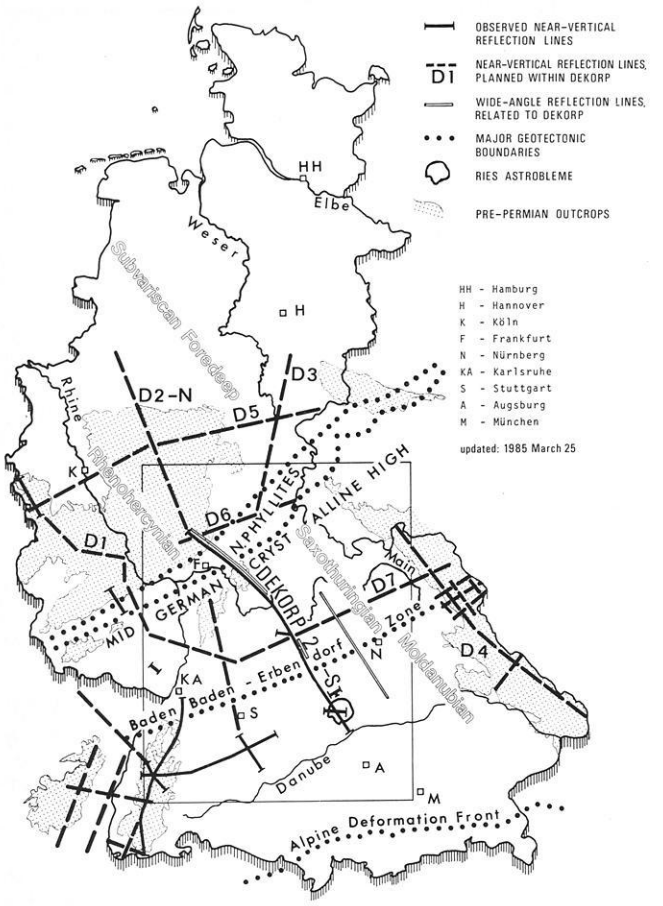

Fig. 1. Location map of observed and planned near-vertical reflection lines in the German Variscides

members from universities, industry and geological surveys. The execution is controlled by a project management group. The field work is carried out by a contractor and various groups of scientists from universities and geological surveys. Most of the data processing is done at the DEKORP Processing Center (DPC) at the Technische Universität, Clausthal. The detailed planning of the profiles and the interpretation of the results is performed by regional working groups set up by the steering committee. Also various scientists of research institutes are working on the data in order to improve methods of processing and analysis. Each year the results are presented at a DEKORP workshop. The entire project is under the auspices of the Geological Survey of Lower Saxony (NLfB), Hannover, and is financed by the Ministry of Research and Technology (BMFT), Bonn.

1.2 Profile DEKORP 2-S and the accompanying seismic activities

The first DEKORP line with a total length of 250 km was observed between April 4 and May 17, 1984. It represents the southern part of the central cross-strike profile called DEKORP 2-S(outh).

From the Danube in the SSE to the Taunus mountains in the NNW, it crosses the Ries astrobleme, the boundary between Moldanubian and Saxothuringian, the Spessart

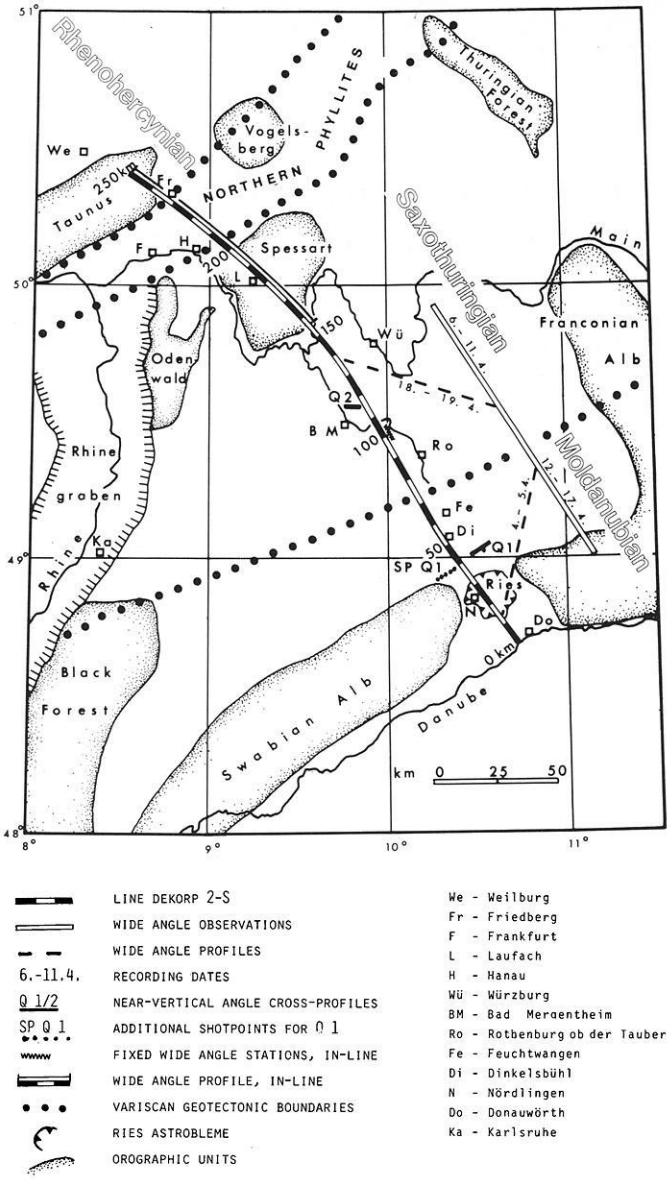

Fig. 2. Location map of the DEKORP 2-S main profile and related seismic measurements

mountains, the Hessian trough and the boundary between Saxothuringian and Rhenohercynian. Figure 2 shows the location map of DEKORP 2-S and the sites of the additional observations to be described later. With exception of a 5-day-experiment with VIBROSEIS in the northern Spessart, explosives in shallow boreholes were used throughout the operation as sources of seismic energy. Charges of 30 kg were fired at depths of 30 m. Average spacing between shotpoints was 320 m. Larger charges up to 90 kg were used for every 4th shot in the southern part of the line and for every 10th shot in the northern part in order to provide sufficient energy for the wide-angle observations.

On the receiving side, 24 geophones per trace in a linear configuration with a total length of 80 m parallel to the profile were used. 200 geophone groups with a spacing of 80 m resulted in a 16 km long geophone spread corresponding to a 1:2 ratio with regard to the relation between spread length and investigation depth, thus providing a basis for the calculation of crustal velocities and a theoretical 25

fold coverage in the subsurface. Data were digitized, multiplexed and telemetrically transmitted by a 16 km long cable to the recording truck. The field work was performed by Prakla-Seismos GmbH, Hannover; the recording unit was a 200 channel Sercel SN 348. For the communication between the up to 100 members of the field crew special transmitter and relay stations had to be installed along the profile.

The additional seismic measurements to be described in detail in chapter 4 consisted of

- Near-vertical observations along perpendicular and oblique reflection spreads in the vicinity of the main profile by means of reflection equipment of university institutes and other research institutions (Sect. 4.1; Fig. 2, profile Q_1 and Q_2).
- In-line wide-angle observations along the main profile by means of conventional reflection equipment (Sect. 4.2).
- In-line and off-line wide-angle observations with portable refraction stations. In the southern part of the DEKORP line a specially stacked wide-angle profile parallel to the main profile has been constructed and, moreover, some in-line observations with fixed stations have been carried out (Sect. 4.3). In the northern part of the profile semi-continuous in-line observations were performed (Sect. 4.4). 80 observers mainly from universities took part in these accompanying observations.

A comparative test using explosives and Vibroseis simultaneously along the same part of the main profile was performed in the crystalline part of the Spessart. Although the use of explosives provided a higher signal to noise ratio for a given coverage than the Vibroseis method, the quality of the Vibroseis record section was considered sufficient to warrant a successful use of the Vibroseis source in future deep reflection surveys, especially in view of a significant improvement by means of higher coverage. On the basis of this experience the Vibroseis technique was chosen for the deep reflection presite survey of the KTB location "Black Forest" in autumn 1984. Also many parameters (e.g. sweep characteristics and number of vertical stacks) tested in the Spessart could be used immediately in the Black Forest and yielded good results.

1.3 Geological situation and objectives of profile DEKORP 2-S

It was the immediate goal of our studies to investigate the crustal structure of the Saxothuringian Zone (ST) and of its transition into the adjacent Moldanubian (MN) and Rhenohercynian Zones (RH) of the Variscan Belt. Today's definition of these zones on the basis of their distinct tectonothermal evolution originally goes back to Kossmat (1927, see also Behr et al., 1984).

The RH is characterized by its continuous sedimentary cover of a mildly folded northwest-facing Paleozoic sequence that is anchimetamorphic or just reaches a very low grade of metamorphism.

The ST exhibits a structural pattern of high mobility. The zone contains remnants of an Upper Proterozoic to Lower Carboniferous cover of varying vergence and generally of very low to medium grade metamorphism together with largely allochthonous polymetamorphic inliers, some of them including granulites and high pressure eclogites.

Most of the MN is made up of polymetamorphic high grade gneisses pervaded by a multitude of late to post-

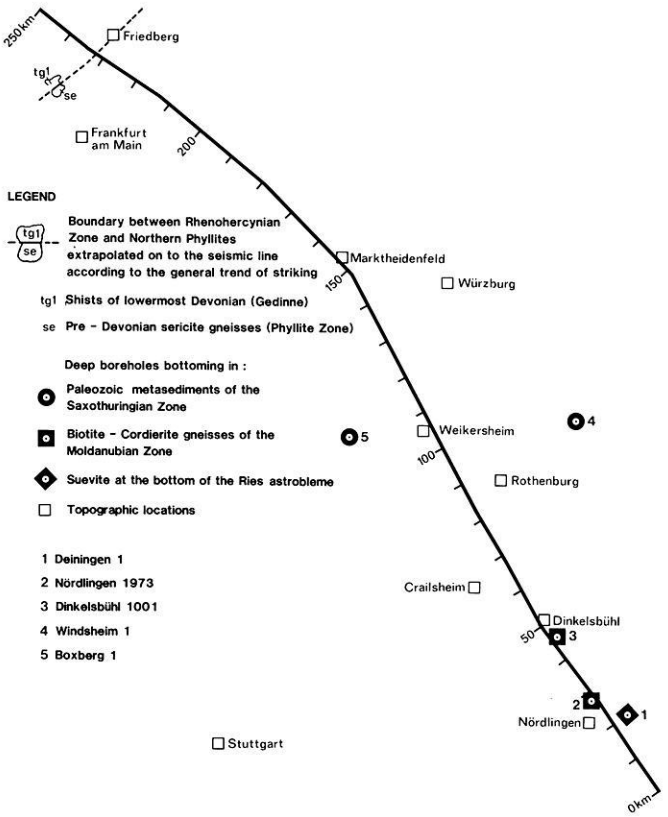

Fig. 3. Location map of important drillings confining the position of the suture between Moldanubian and Saxothuringian zone

kinematic granitoids. Its relic suprastructure consists of usually slightly deformed paleozoic sediments.

During the last decade the concepts of nappes and horizontal tectonics for the RH-, ST- and MN-Zones of the Variscan belt have been revived (Ziegler, 1978; Martin and Eder, 1983; Behr et al., 1984). Certainly, also near-vertical normal faulting is observed along the profile, and for quite a long time it has been attempted to explain the Variscan tectonic processes as mainly vertical tectonics with no considerable crustal shortening. It is one of the main subjects of this seismic experiment to obtain as much evidence as possible about the crustal structure in this area in order to support or modify the current geological concepts of the tectonics of the Variscan belt.

DEKORP 2-S traverses the Franconian Platform (Carlé, 1955; Ziegler, 1982) from south of the Ries astrobleme toward northwest ending beyond the northeast branch of the Rhine Graben within the Taunus mountains. Along the seismic line the Variscan is covered by up to 1.6 km of Permian and younger sediments except for the Ries, the Northern Spessart and the Taunus mountains. Within the Ries astrobleme the impact excavated crystalline basement slivers of the Moldanubian Zone. In the Northern Spessart late Variscan uplift and Tertiary rejuvenation exposed a segment of the ST that represents part of the Mid German Crystalline High (MGCH). Similar processes led to the exposure of the southern margin of the RH in the Taunus mountains at the northern end of the profile.

Additional information from deep wells penetrating the Mesozoic platform cover constrains the approximate position of the MN-ST boundary to between kms 45 and 85 of the profile (see Fig. 3), whereas the RH-ST boundary

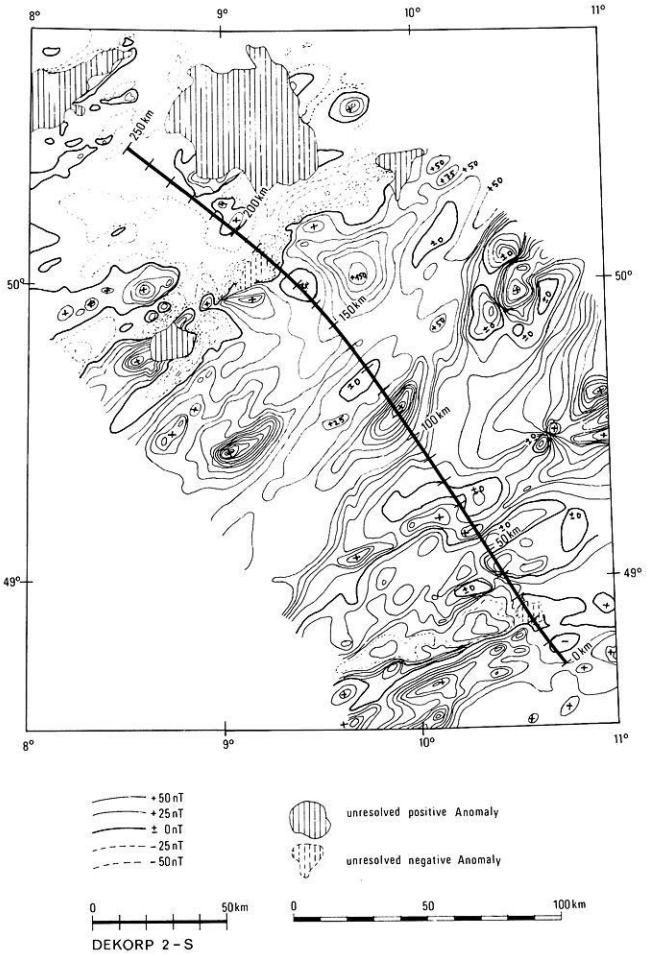

Fig. 4. Location of DEKORP 2-S with adjacent anomalies of the total magnetic intensity. Note that between km 50–100 isolines with an interval of 5 nT are added. From: Aeromagnetische Karte der Bundesrepublik Deutschland 1:1.000.000 (Eberle, 1973) and Karte der Anomalien der Totalintensität des erdmagnetischen Feldes in der Bundesrepublik Deutschland 1:500.000 (Bundesanstalt für Geowissenschaften und Rohstoffe, 1976)

is extrapolated from nearby outcrops to occur close to km 233 beneath Lower Permian of the Hessian trough and Tertiary sediments of the NE branch of the Rhine Graben.

The following is intended as a brief outline of the geological evolution of the study area.

ST sediments exposed, among others, in the Bohemian Massif and Thuringian Forest indicate an Early Paleozoic basin with a shallow carbonate platform to the south. Ordovician and younger bimodal volcanism suggests an early development of this ST basin on rifted crust, the southern fringe of which was affected by the Ligerian Convergence at the turn of the Silurian-Devonian.

A restricted deep water basin persisted to the north which itself was bounded in the north by the MGCH, emerging probably from the mid-Devonian onward. The final destruction of the ST basin occurred during the Sudetic convergence probably from 330 my onward following the inferred closure of the basin of the Northern Phyllites. According to current concepts (Behr et al., 1984) to be tested by DEKORP, the convergence is an expression of the northward migration of an orogenic front lasting from Ordovician to Carboniferous times and being driven by a southward subduction of continental lithosphere (Ziegler, 1978).

During late Carboniferous and the Early Permian the post-Variscan collapse led to the formation of intramontane basins whose depocenter alignments were largely controlled by the Variscan structural trend notwithstanding an as yet unproven contribution of late-Variscan wrench faulting to their development (e.g. Arthaud and Matte, 1975). DEKORP 2-S crosses two of these NE trending basins, namely the Oos-Stockheim trough (Carlé and Wurm 1971), extending between kms 100 and 170, and the Hessian trough (Falke, 1971) between kms 200 and 235.

Also, the thickness of lower Permian strata preserved below marine Zechstein as deduced from reflection seismics and deep wells (Trusheim, 1964) indicates that the amplitudes of intra-Rotliegend down-faulting and warping did not exceed 900 m in the Oos-Stockheim trough or 600 m in the Hessian trough.

The Mesozoic cover of the Franconian platform was deformed along preexisting discontinuities as the whole Platform is pervaded by faults of Hercynian and Rhenish trends.

Particularly toward the NE of the platform the Hercynian faults exhibit strongly compressional geometries. Some of them were active during the Permian with throws partly exceeding 1,000 m. They were reactivated from the Lias onward and persisted probably to the Late Tertiary.

By contrast, faults with Rhenish trends are concentrated in the western segment of the platform. They exhibit mainly extensional geometries or intermittently left-lateral slip. They were active mainly from Eocene to Holocene and probably accompany the formation of the Central European Rift System in its Bresse-Rhine-Leine-Segment.

This intra-platform deformation largely attributable to the Alpine cycle affected the area of the DEKORP 2-S line only by a slight warping with amplitudes up to about 100 m (e.g. Carlé, 1955). One of the latest events to affect the area under investigation was the Ries impact about 15 my ago. It led to the excavation of a shallow crater about 25 km in diameter. Earlier refraction seismic observations demonstrated brecciation of the Moldanubian basement down to at least 4 km below the crater floor (Angenheister and Pohl, 1969, 1976).

The position of the profile referring to magnetic and Bouguer gravity anomalies is shown in Figs 4 and 5, respectively.

With regard to the MN/ST boundary a straight chain of small magnetic anomalies exhibiting their maxima in the south and their minima in the north of the boundary is observed, crossing DEKORP 2-S at about km 75. In Fig. 5 this zone coincides with the southern margin of a major positive Bouguer anomaly, the Neckar-Tauber anomaly.

In the interval between km 100 and km 140 two positive magnetic anomalies are crossed which belong to magnetic lineaments striking N 45° E. These lineaments can be followed from the Main river to the Vosges mountains, at least. The southern one crosses the Haslach area in the Black Forest. The tops of the corresponding bodies beneath the profile DEKORP 2-S are not deeper than 5 km. In the neighbourhood of the profile both magnetic lineaments are running parallel with positive Bouguer gravity anomalies. Thus, it can be concluded: along the MN/ST boundary there are relatively small magnetized bodies situated on the MN side. In the area along the profile from its southern

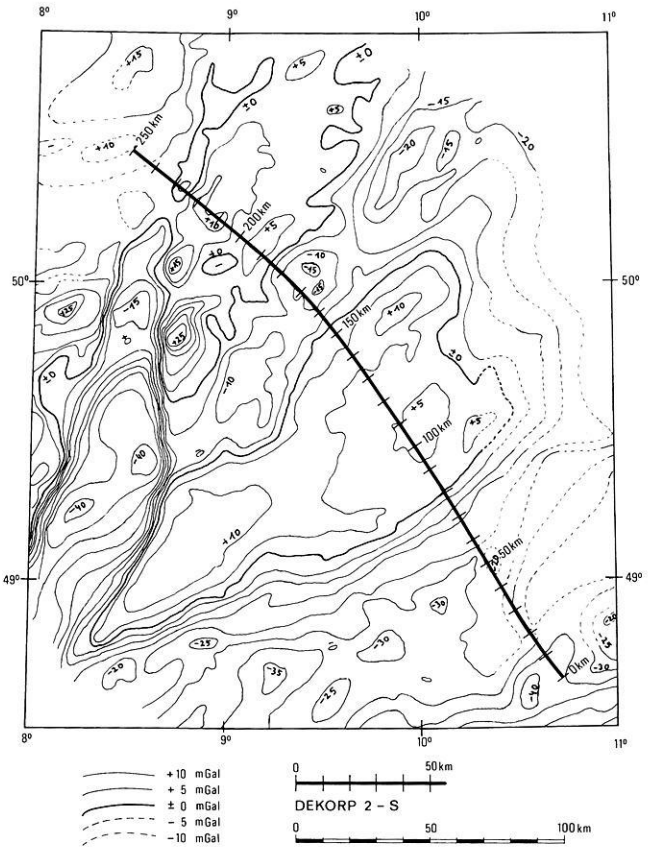

Fig. 5. Location of DEKORP 2-S with adjacent Bouguer anomalies of gravity. From: Schwerekarte von Westdeutschland (Gerke, 1957)

boundary to km 150 the ST shows a higher average density and a stronger average magnetization than the MN north of the Nördlinger Ries.

Between km 155 and km 185 the profile crosses a band of negative Bouguer anomalies striking about 45° N. It runs along the outcrop of the Middle and Lower Bunter from the Rhön mountains to the Odenwald. In the area crossed by the profile the gravity minimum line coincides with a magnetic minimum. At km 178 the profile enters a zone of strong negative magnetic anomalies. They are arranged in an irregular band some 15 km wide with a general strike direction of 50°–60° N. It seems to indicate a large magnetized mass being located south of this band and having its northwestern edge along the zero-line of the anomalies with a steeply dipping boundary face; the top should be outcropping or subcropping. The Bouguer gravity map shows in this interval (km 178–193) only a weak increase towards a maximum at km 210.

At the western border of the Hessian trough at km 225–230 a weak gravity minimum is situated. The magnetic isolines beyond km 193 do not show any remarkable anomalies.

One of the objectives of DEKORP is to better understand the causes of the gravity and magnetic anomalies, too.

1.4 Organization and techniques of the field survey

The near-vertical reflection measurements along the profile DEKORP 2-S were performed using explosives. The decision to do so was based on two reasons:

Table 1. Field parameters for near-vertical reflection measurements

Equipment	SERCEL SN 348, telemetric, 200 traces
Sampling rate	4 m s
Record length	20 s
Low cut filter	8 Hz, 18 db/oct
High cut filter	62.5 Hz, 72 db/oct
Preamplification	$2^4 = 24$ db
Number of geophone groups	200
Spacing of geophone groups	80 m
Geophone pattern	24 fold, in-line
Pattern length	80 m
Shotpoint spacing	a) 320 m (near vertical angle) b) 1,280 m (wide angle)
Depth of charge	30 m
Size of charge	a) 30 kg, partly reduced to 5 kg (near vertical angle) b) 90 kg, partly reduced to 60 kg (wide angle, every 4th or 10th shot, resp.)
Spread	off-end-shooting
Spread length	15.92 km
Offset	
1. in-line	a) 40 m (near vertical angle) b) 57 km (wide angle)
2. off-line	max. $\pm$ 500 m
Coverage	a) 25 fold (near vertical angle) b) 6 fold (wide angle)

– No experience had been collected so far in Germany with the Vibroseis method for deep crustal studies outside the large sediment basins.
– The observations in the wide-angle range by university groups made the use of explosive sources necessary because Vibroseis cannot be recorded properly by the equipments of the institutes. Thus, the additional observations could be well integrated into the continuous profiling work of the contractor along the main profile.

Table 1 displays the most important field parameters. The maximum shot-receiver distance of 16 km was chosen in order to get reliable information about the crustal velocities. The in-line 80 m long geophone pattern should have been approximately twice as long because analysis of noise waves has yielded wave lengths of up to 300 m; by a geophone group setup of 160 m and by twofold vertical stacking during the processing procedure wave lengths up to 320 m could have been extinguished. On the other hand, the chosen setup provided a simple and economical way for laying out and collecting geophones within just one trace interval.

Preparations for the measurements started two months ahead with geodetic surveying and permitting. The measurements began in the south on April 4, 1984, rolling along to the north, and ended on May 17, 1984 after 32 working days and a break between April 19 and May 2. For economical reasons a progress of 10 km per day was considered an optimum. The contractor's crew was increased to 103 persons for the continuous profiling plus 28 persons for the Vibroseis experiment and 6 persons for the wide-angle shots. Up to 16 drilling rigs were in operation simultaneously.

The prerequisite for the intended progress was a careful planning and a tight organizational schedule, especially in view of the rough terrain in the Spessart and in the Taunus mountains. Serious drilling problems arose by the presence

of massive limestones of the Muschelkalk formation and of hard gneisses and quartzites in the crystalline part of the Spessart. These difficulties were overcome by the in-hole hammering technique.

An important condition for a smooth operation was a reliable radio-communication between all participating groups, sometimes operating at distances of up to 80 km in rough terrain and tamber forests. Up to 6 moving relay stations were in operation simultaneously.

In spite of all these problems and poor weather conditions with ice and snow at the beginning of the measurements, the progress of 10 km per day turned out to be achievable on the average. On 26 working days 729 shots were fired along the 250.8 km long profile. 11% of the planned shotpoints had to be discarded for security reasons, reducing the mean coverage from 25 to 22. On the average, 28 shots were fired on a 10-hour working day with an average line progress of 9.62 km per day.

2. Data processing of the main profile

A first preliminary treatment of line DEKORP 2-S has been carried out at the DEKORP-Processing-Center (DPC) in the Geophysical Institute of the Technische Universität, Clausthal.

For data processing a seismic computing system – type: Phoenix I – was at disposal, hardware consisting of a Raytheon minicomputer – type: RDS 500 (64 K × 16 bit core memory) – with floating point and array processor. Mass storage was provided by 4 Wangco tape units (75 ips, 1,600/800 bpi) and by a CDC disk unit (80 Mbyte). The appropriate software comprises a multitude of programs for analysis, processing and display of seismic data so that all standard procedures customary in exploration seismics can be applied.

In the following each step of the processing and its importance especially with regard to deep seismic data processing will be explained. Also the first steps of more refined processing procedures on profile DEKORP 2-S – not yet completed – are described.

2.1 Common shotpoint gathers

Scaling. In a first step the samples had to be rearranged from a time-multiplexed into a trace-sequential format (demultiplexing), yielding common shotpoint gathers. The Sercel equipment compensates automatically for the large dynamic range of about 120 dB of the movement of the ground by instantaneous floating point recording. This procedure has been retrieved in order to get true reflection amplitudes (amplitude recovery). Figure 6a shows the result. Due to the extremely high differences between amplitudes at the beginning and at the end of the seismogram practically only the first arrivals and the strong surface waves are recognizable in Fig. 6a. Then, the amplitude values have been multiplied by the factor $k \cdot T \cdot e^{aT}$ (where k = const., T = traveltime and a = constant of absorption) in order to compensate for the systematic amplitude decrease due to spherical divergence ($\sim 1/T$) and absorption ($\sim e^{-aT}$) and to obtain a balanced seismogram. The value of a has been assessed empirically for processing purposes only and has no direct physical meaning.

In order to find suitable values for a and k by least squares fitting numerous analyses of energy in single records along the profile have been carried out. The best result is obtained when at 5 s two way traveltime (TWT) the exponential function is replaced by a constant value because from thereon a constant noise level is prevailing. Typical values of a cover the range from 1.1 s^{-1} to 1.8 s^{-1}. An exception is represented by the Nördlinger Ries data where a reduction to 0.8 s^{-1} is observed.

In order to correct for influences of coupling between ground and geophone or shot, respectively, a constant scaling factor for each trace has been applied to get the same root mean square energy for all traces (trace equalization). Figure 6b shows an amplitude-corrected shot with a uniform energy behaviour.

Data quality. Part of the recorded seismograms exhibits a high noise level by technical reasons or by field conditions. A first quality control has been provided by monitor playbacks in the field.

According to the type and strength of the noise one of the following methods has been chosen for noise discrimination: frequency filtering, partial zeroing, change of polarity or complete elimination of traces.

In order to discriminate first arrivals and other undesired waves initial muting of traces extends from about 200 ms (near the shotpoint) to 6–9 s (at the end of the spread).

On the other hand, the low frequency high energy surface waves (Fig. 6b) often coincide with reflections and cannot be muted. Even by low-cut filtering, only a weakening can be achieved because the frequency spectra of the surface waves (about 5–20 Hz) and of the reflections (about 10–40 Hz) overlap. Figure 7 exhibits that this holds true especially for near-shotpoint traces and in the first few seconds. Since surface waves were sufficiently weakened by stacking, time consuming procedures for their elimination, e.g. wavenumber filtering, were not applied in the first preliminary data processing.

In Fig. 8a completely processed common shotpoint gather is shown with the muting curve used. It contains a few distinct reflections and many strong diffractions, above all. All common shotpoint gathers have been plotted at the DPC. Data quality – except in the above mentioned cases – is good. Along the major part of the profile reflections are scarce in the upper crust and a distinct beginning of strong energy at about 5 s TWT is observed. A better resolution of the weak reflections in the early traveltime range makes special processing necessary.

Common-midpoint-sorting. Sorting of common shotpoint gather data into common midpoint gather data (CMP) was performed on the basis of geodetic data made available on magnetic tapes. The intended coverage on profile DEKORP 2-S was 25 fold. Therefore, every 4th receiver point was used as shotpoint location for the given spread. Shots cancelled by security reasons and the elimination of noisy traces yielded a real coverage of 20–22 fold after editing and sorting. Extreme values of coverage along the profile were 9 and 31, respectively. The product of 200 traces per record, 5000 samples per trace and more than 20 fold coverage in connection with the small capacity of disk storage at the present computing equipment made CMP gathering the most time consuming step of the processing.

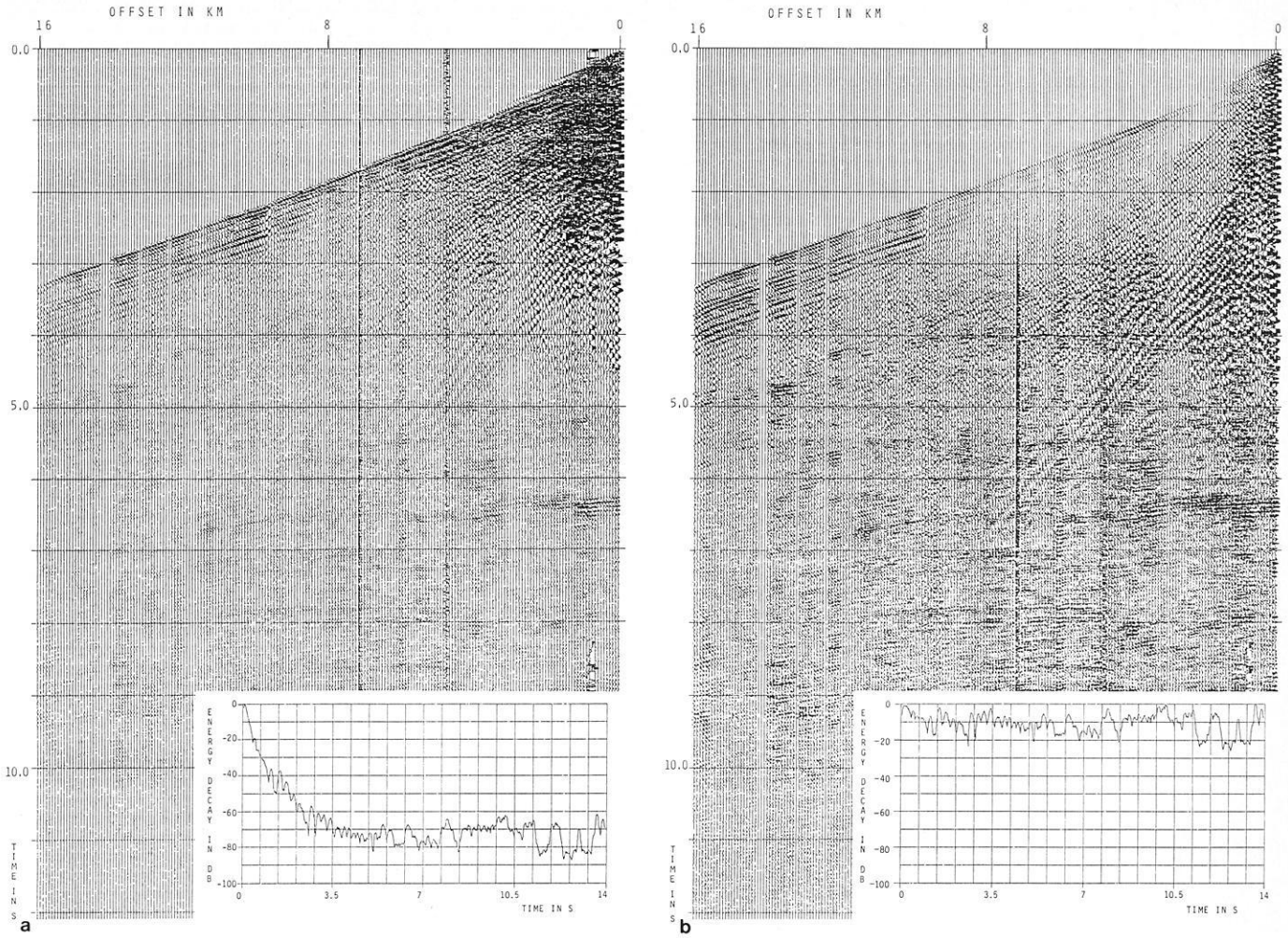

Fig. 6. **a** Common shotpoint gather before correction by analytical gain function, i.e. true amplitudes are shown. In the *lower part* of the figure the time dependent energy behaviour is shown; **b** Common shotpoint gather after correction by analytical gain function. In the *lower part* of the figure the time dependent energy behaviour is shown

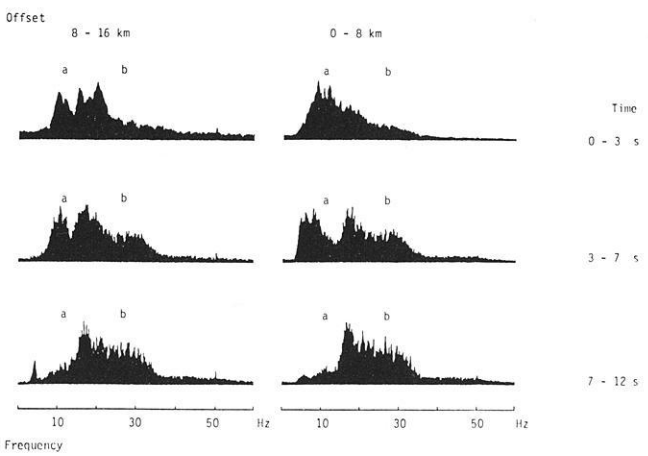

Fig. 7. Amplitude spectra of a common shotpoint gather averaged in time and space for different offset ranges: (*a*) surface waves, (*b*) signal

2.2 Common midpoint gathers

Static corrections. Static corrections have been calculated from uphole times and from topographic elevations by the field crew. In order to obtain the correction velocities and to interpolate between shotpoints the first arrivals up to distances of 2 km or more have been used. The datum level was chosen to be 400 m above seal level. The removal of the uppermost layers with low velocities has been performed in most cases down to the first high velocity layer. Hence, low velocity layers below the limestones of the Malm or Muschelkalk in the southern part of the profile have not been taken into account. In the Nördlinger Ries the "Seeton" (limnic) sediments have been corrected for, only, but not the Suevite which is characterized by medium velocities.

With regard to future processing of data, especially more subtile velocity analyses, it is planned to evaluate all first arrivals up to the maximum offset of 16 km and to compensate for lateral variations of velocity down to some km depth by seismic stripping. In the region of the Nördlinger Ries appropriate velocity models are already available.

Deconvolution. The optimal parameters for deconvolution have been estimated by calculation of autocorrelation functions and amplitude spectra. The tests resulted in a prediction length of 4 ms (spike deconvolution), and by noise

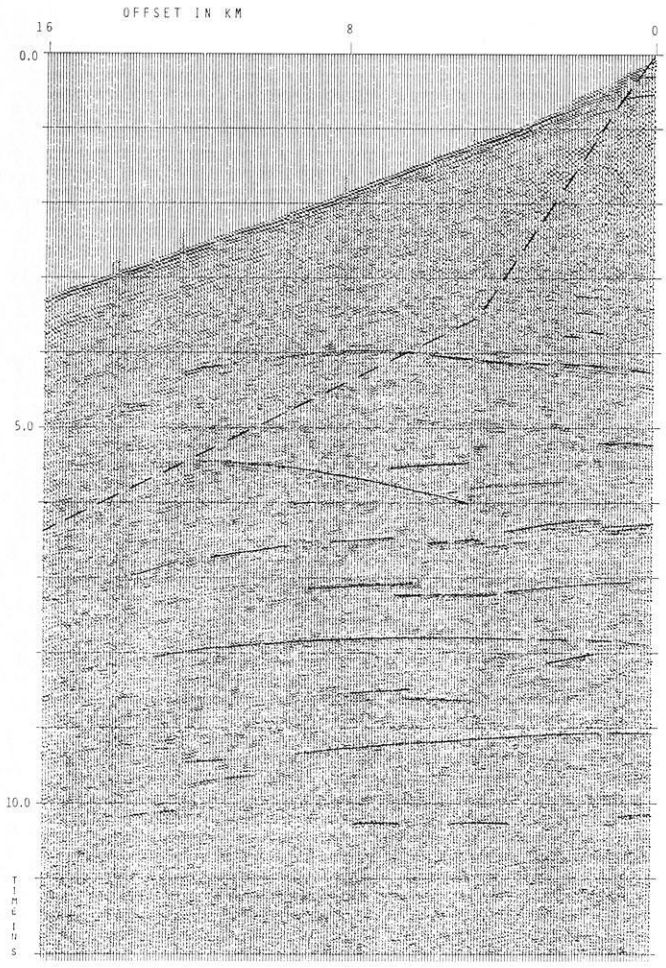

Fig. 8. Common shotpoint gather of Fig. 6b after frequency filtering and scaling (AGC) with interpretation and with muting curve (*dashed*)

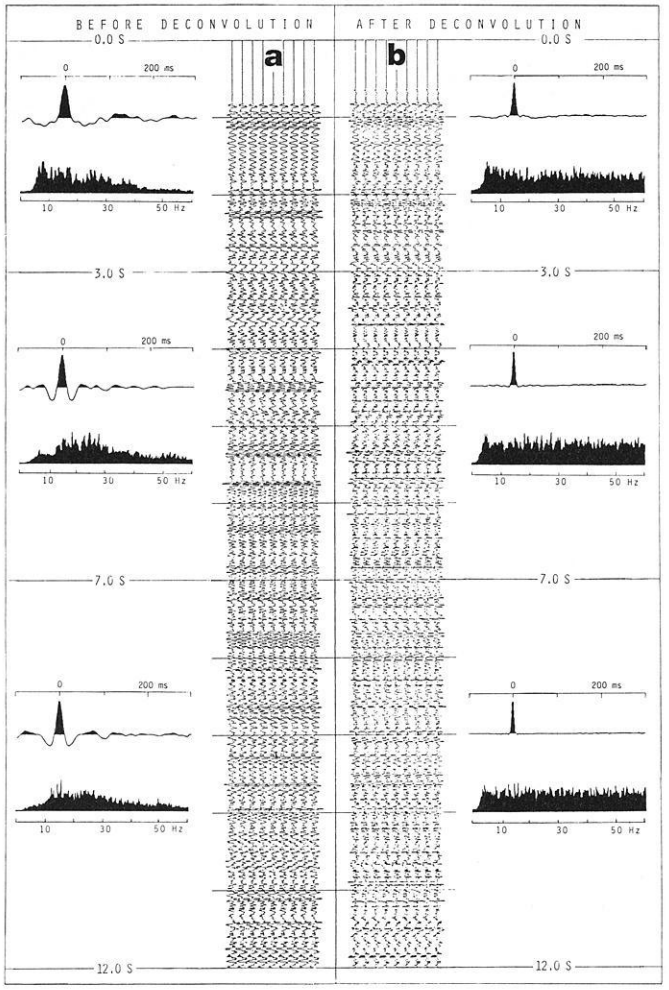

Fig. 9. a One trace of a CMP (repeated 9 times for better readability) with the corresponding autocorrelation functions and amplitude spectra summed over all CMP traces in three different time windows before deconvolution. **b** The same as in **a**, but after deconvolution

mixing of 0.2% steady state inverse filters with operator lengths of 120–180 ms were obtained. Figure 9a shows one trace of a CMP gather before deconvolution with the corresponding autocorrelation functions and amplitude spectra summed over all CMP-traces in three different time windows. Figure 9b shows how the long seismic signals have been contracted after deconvolution. The side lobes of the autocorrelation functions corresponding to the amplitude maxima and minima of the signal have disappeared. The rest is a narrow central maximum indicating a statistical series of reflecting signals. The amplitude spectra are nearly whitened corresponding to the appearance of spike-type signals in the time traces. By subsequent bandpass filtering the pulses have been transformed into (symmetrical) zero-phase signals.

Dynamic corrections and CMP stacking. In order to estimate stacking velocities stacking tests have been carried out every 3 km along the profile with groups of 11 CMP's applying 48 constant velocities. An important problem was posed by the appearance of numerous diffractions (see Fig. 8). The optimal stacking velocities for diffractions are higher than those for subhorizontal reflections. Because diffractions prevail by number and by energy the recovery of the weaker reflected events in the stacking tests of 11 CMP's often was difficult. Frequently two or three stacking maxima (see Fig. 10) are observed, when diffractions appear beside reflections. In addition problems arise by different dips of reflecting elements. In order to improve the classification of the seismic signals stacking tests with a greater number of CMP's are being performed. This work has not been finished, yet.

The deviation of reflection traveltime curves from ideal hyperbolas is very slight in our case despite the maximal offset of 16 km. It has been shown by calculations that this deviation amounts to only 12 ms at 16 km offset for reflections from 10 km depth, and for 30 km depth the result is 3 ms. These values correspond to less than half a wavelength in the observed frequency range. The reason is that the vertical gradient of the velocity is very small which implies that the effects of refraction cannot be very strong. Therefore no difficulties can arise with regard to the stacking procedure. On the other hand, problems are encountered by the length of the spread in connection with lateral variations of the geological conditions close to the surface.

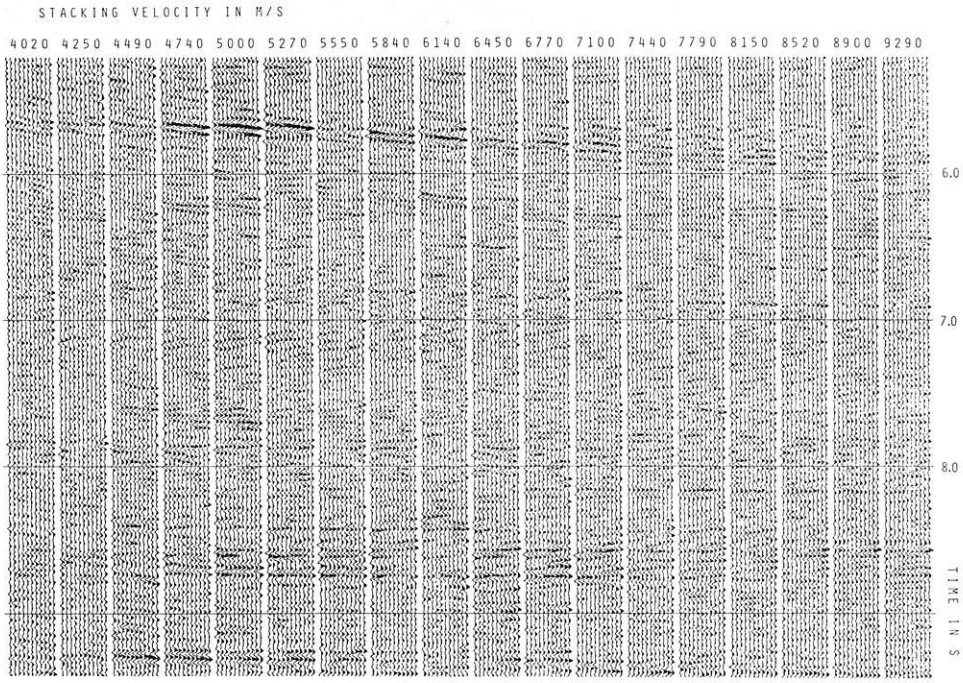

Fig. 10. Part of a velocity analysis (constant velocity stack). Note the multifold alignments for different velocities. Correction velocities are given on *top* of the figure

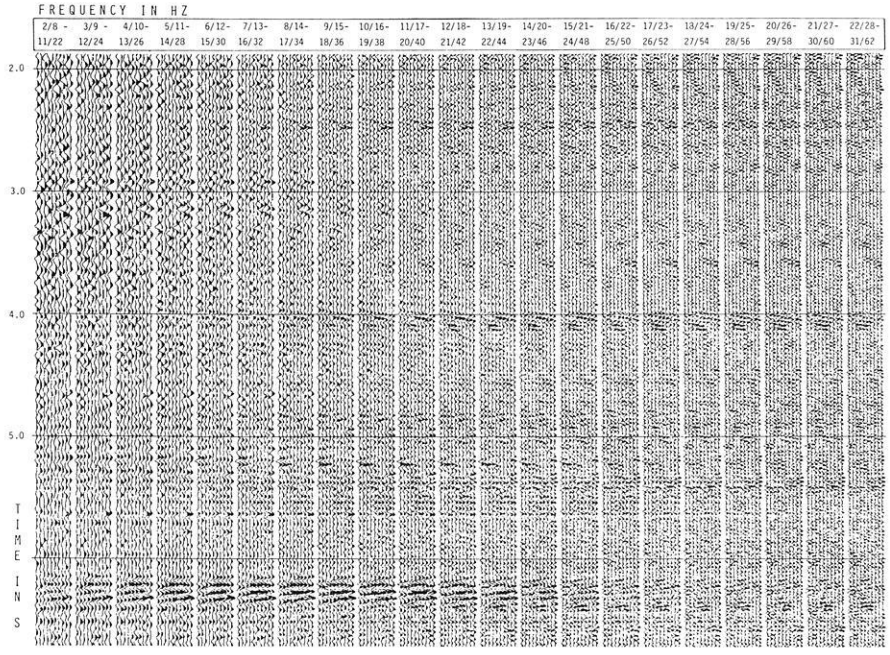

Fig. 11. Part of a filtertest (stepwise shifting of a narrow bandpass of constant width over the entire frequency range). Filter characteristics are given on *top* of the figure

2.3 Stacked section

Frequency filtering. After scaling (AGC) and stacking different bandpass filters have been tested by application on groups of 10 CMP's which are representative for a larger part of the profile. Two ways have been used in order to get the optimum filter parameters:

– Stepwise shifting of a narrow bandpass of constant width over the entire frequency range yielding the main frequencies of the reflections.

– variation of the low cut-off frequency, fixing the high cut-off frequency, and vice versa yielding the low- and high-cut boundaries.

Figure 11 shows part of a filter test after the first method. The main frequencies of the signals are in the ranges 12–30 Hz for shorter traveltimes and 6–24 Hz for longer ones. Therefore, it was necessary to choose the shape of the trapezoidal bandpass filters carefully. Figure 12 shows the average filter parameters used. A stacked and filtered time section is shown in Fig. 20; such sections represent an essential basis for the interpretation.

Migration. As a last step a migration of the entire profile was performed. Along km 24–72 of the profile the Kirchhoff-, finite-difference-(FD-) and frequency-wavenumber-(FK-) migration methods have been tested. The FD-migra-

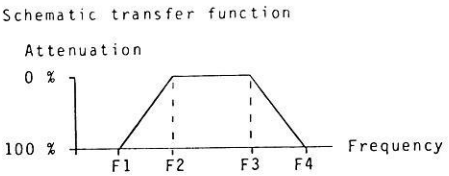

Time interval in s	Characteristic filter points F1 F2 F3 F4 in Hz
0 - 2.2	8 / 15 - 20 / 40
2 - 5	6 / 12 - 19 / 38
4.5 - 11	4 / 9 - 18 / 36
10 - 20	3 / 8 - 16 / 32

Fig. 12. Sketch of bandpass characteristics and table of bandpass limits used (averages)

Table 2. Velocity vs. Time function used for migration (v_{rms} = RMS velocity; v_{int} = interval velocity)

TWT (s)	v_{rms} (m/s)	v_{int} (m/s)
0.0		
		3,500
0.5	3,500	
		4,720
2.5	4,500	
		6,040
6.5	5,500	
		7,240
10.3	6,200	
		8,240
14.0	6,800	

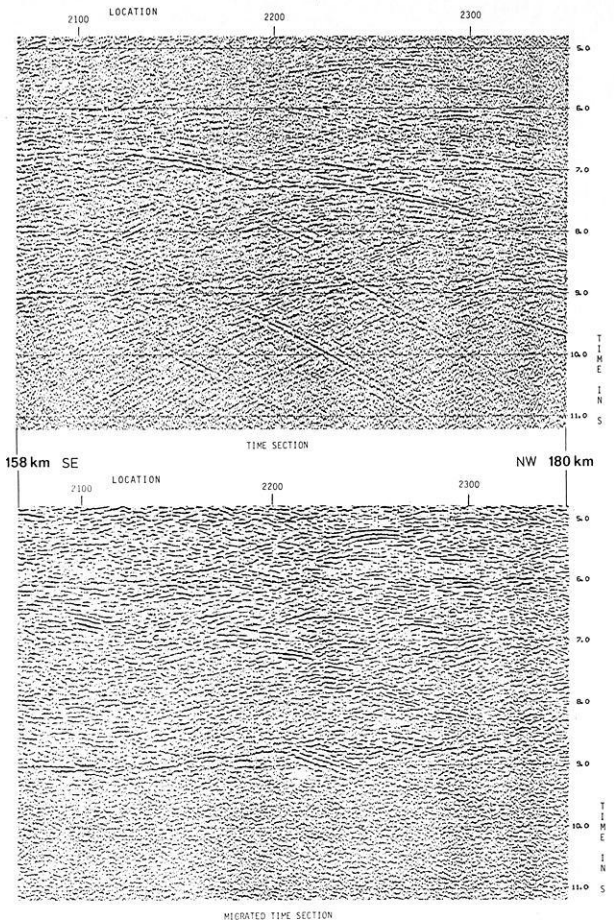

Fig. 13. Part of the DEKORP 2-S stacked section from the Spessart area (km 158–180) before migration (*top*) and after migration (*bottom*)

tion provided the best results with regard to the signal/noise ratio, but it required, unfortunately, the longest processing time.

The interval velocities derived from stacking velocities varied strongly and showed partly too high values. For this reason they could not be used as migration velocities. Therefore an approximate velocity function has been derived from smoothed and reduced stacking velocities and from other informations about the crustal structure (Table 2). This function has been used for the entire profile. The resulting section is shown in Fig. 23 and is compared with another migration by the same method shown in Fig. 22.

Because of the restricted computer capacity the whole body of data has been resampled with a time increment of 8 ms. No considerable loss of information occurred because of the prevailing low frequencies. Still, the profile had to be migrated in 6 parts. Due to sufficiently large overlapping the boundaries of the single parts match well. A restriction to the first 15 s TWT was economical because below the Moho reflections little useful information is present.

The result is satisfactory for the entire section in spite of the laterally constant velocity function. Above all, the focussing of the diffractions yields a significantly clearer picture for interpretation, e.g. in the Spessart section (Fig. 13).

2.4 Special processing

The standard processing described in the previous sections could not remove all observed and already mentioned difficulties. In the following special processing of selected parts of the profile is presented using three particular examples.

Frequency-wavenumber filtering. The appearance of strong surface waves in many DEKORP seismograms obscured weak reflections in near-surface regions. The overlapping of the frequency bands of signal and noise makes the application of conventional bandpass filtering ineffective in many cases. Frequency-wavenumber filtering is an efficient but also very time-consuming tool for the elimination of noise waves. After 2-dimensional Fourier transformation of the seismograms from the traveltime-distance (t-x) domain into the frequency-wavenumber (f-k) domain the signal amplitudes are obtained in dependence on frequency and apparent wavenumber.

Figure 14 shows the f-k transform of the common shotpoint gather of Fig. 6b. In the f-k spectrum waves with higher velocity are displayed as straight lines with greater slope than those with lower velocity. Therefore, refractions ($v = 5{,}000$ m/s) can be clearly distinguished from surface waves ($v = 1{,}600$ m/s). Both wave types appear only on the left side of the figure because of the single-sided spread configuration. Steep angle reflections show up as a point cluster around $k = 0.0\ m^{-1}$ and $f = 18.0$ Hz. Due to the relatively large geophone group interval (80 m) spatial aliasing appears, for $v = 1{,}600$ m/s even from 10 Hz on.

If the f-k spectral parts above the dashed filter limits

in Fig. 14 are rejected (i.e. all waves with $v < 3{,}600$ m/s are suppressed) a complete elimination of surface waves in the x-t domain is achieved (see Fig. 15).

It is not reasonable to restrict the bandpass in the f-k domain further, because the reflection hyperbolas could be affected which exhibit also steeper slopes at greater offsets. Therefore, the refraction arrivals have to be removed by appropriate muting in the common shotpoint gather.

Nevertheless, the f-k filtering of the first 40 km of the DEKORP profile (Nördlinger Ries) did not yield the expected enhancement in the early traveltime range, probably due to the absence of reflections. Considering the fact that the surface waves are already weakened by stacking and considering the uneconomical relation between effort and result it did not seem to be reasonable to process the entire profile in this way.

Nördlinger Ries. From earlier investigations using the reflection seismic method in the Nördlinger Ries very clear reflections from the boundary between limnic "Seeton" sediments and Suevite at about 250–400 ms are known (Angenheister and Pohl, 1969). A comparable result from the DEKORP measurements cannot be expected because due to the spread configuration not even a single fold coverage is obtained in this time range and because the low velocity limnic sediments have been removed already in the correction process as mentioned earlier in Sect. 2.2. The following steps were made in order to reveal the base of the limnic sediments: (1) Careful editing of bad traces, (2) application of f-k filtering in order to eliminate the surface waves especially in the Ries, (3) selection of an optimal interpolated muting curve in order to retain maximal coverage and (4) replacement of the "Seeton" corrections. Thus, a clear enhancement was achieved: The base of the limnic sediments is more clearly recognized now (see Fig. 16).

In summary it must be stated that it is not possible to resolve simultaneously the near-surface geological units as well as the deeper subsurface especially if distinct lateral velocity inhomogeneities occur as observed in the Ries. The resolution of structures in the lower crust makes necessary deeper reaching seismic stripping or undershooting of the inhomogeneous near-surface areas by means of a different spread configuration.

True amplitude stacking. The automatic gain control (AGC) applied before and after stacking implied the loss of true reflection amplitudes in favour of a balanced seismogram picture. In order to get an assessment of the real temporal behaviour of energy a so-called true amplitude stack (TA) was performed for the profile range from 77–97 km. In this process the amplitude correction involves only an analytical gain function (correction for spherical divergence and absorption) and a trace equalization (correction for different shot charges and coupling between geophone and ground) but no AGC. Before the derivation of the parameters of the $k \cdot T \cdot e^{aT}$-function and their application on the seismic traces low-cut filters had to be applied in order to suppress strong surface waves.

Further, new muting curves were chosen very carefully in combination with revised velocities. The result of this true amplitude processing is shown in Fig. 17a. For the sake of comparison the same part of the profile has been stacked with predictive deconvolution (16 ms prediction length) and with AGC, too, see Fig. 17b. Whereas conven-

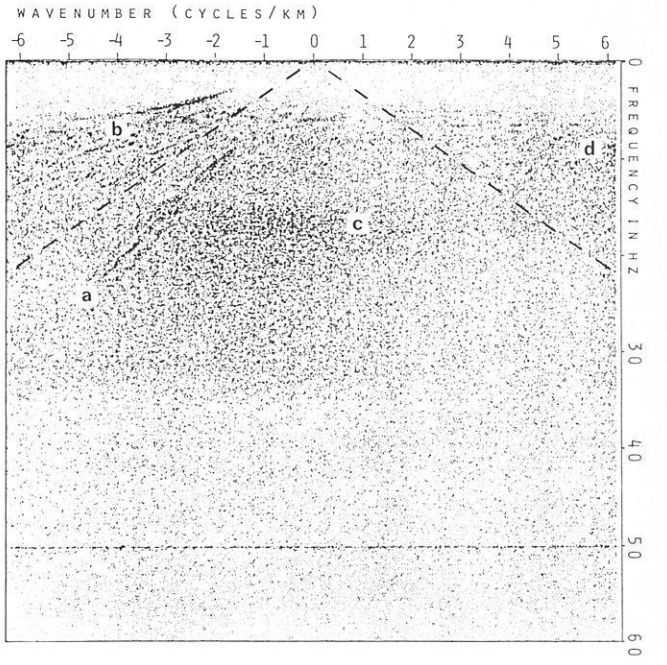

Fig. 14. Frequency-wavenumber (f-k) transform of the common shotpoint gather shown in Fig. 6b: **a** first arrivals, **b** surface waves, **c** signal, **d** aliasing of **b**; *dashed lines* indicate f-k filter limits

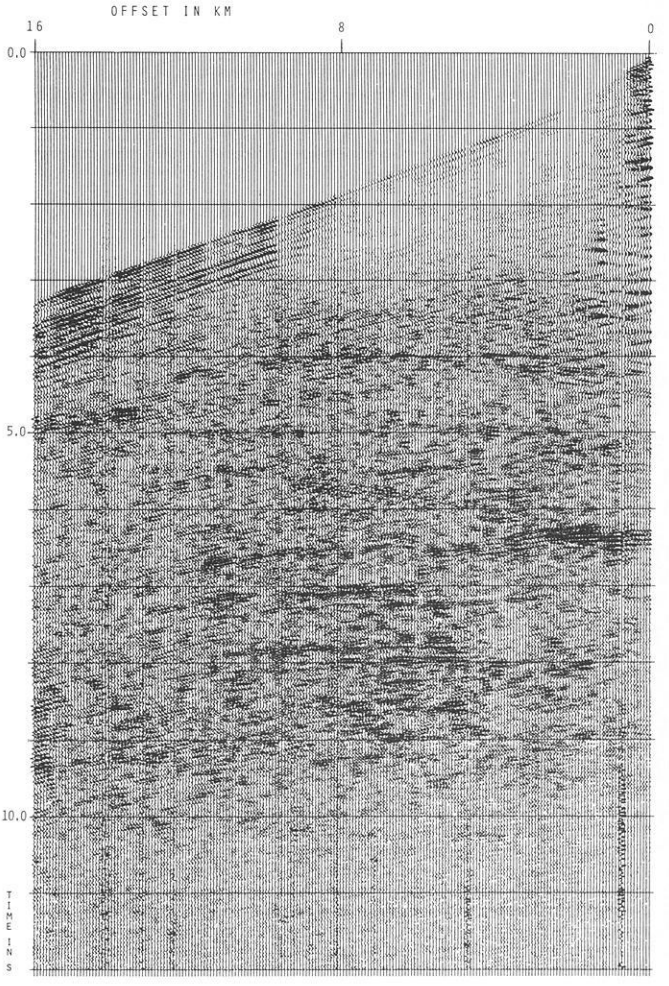

Fig. 15. Common shotpoint gather of Fig. 6b after frequency-wavenumber filtering

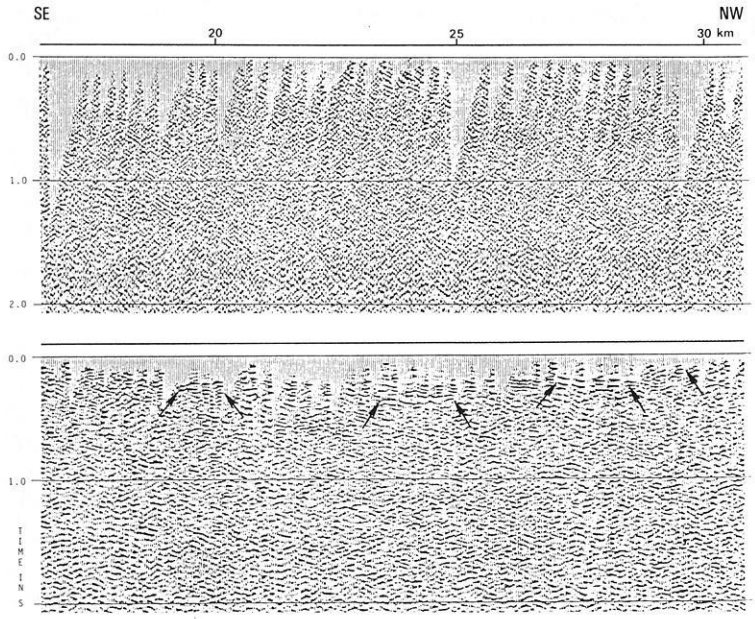

Fig. 16. Part of DEKORP 2-S (Nördlinger Ries). *Top:* first stack. *Bottom:* reprocessed stack with replacement of the limnic ("Seeton") sediments ("Seeton" base is indicated by *arrows*)

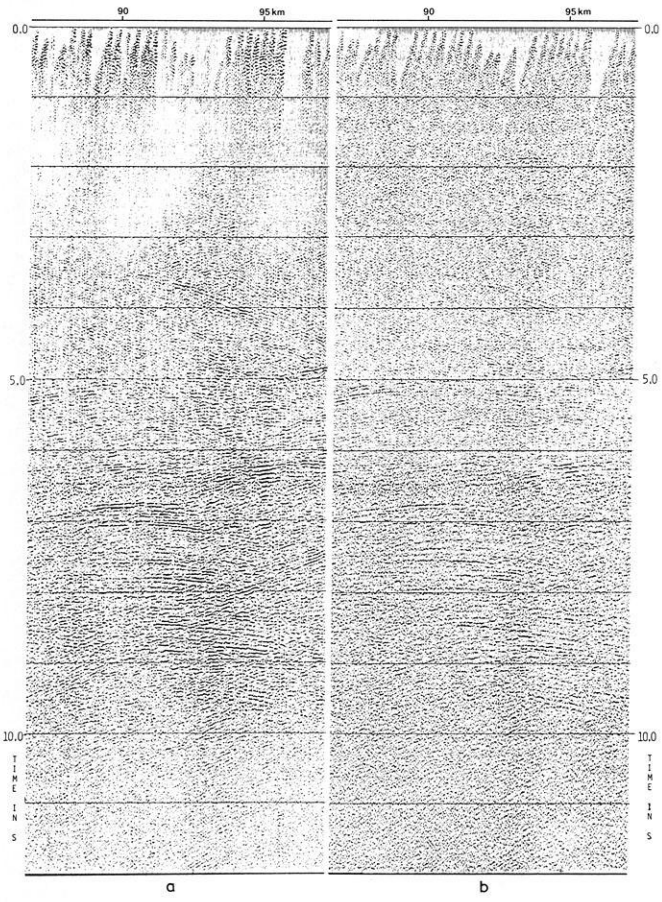

Fig. 17a, b. Comparison of a true amplitude stack (**a**) with a conventionally processed stack (**b**)

tional processing emphasizes all events more or less equally the TA processing shows a high dynamic range. Beside the predominant diffractions only a few reflections with high contrast of impedance are observed. Many weak events can hardly be recognized. The frequency content of the reflections reaches up to 50 Hz.

2.5 The velocity problem

In order to obtain reliable velocity information from the deeper crust a maximum shot-receiver distance of 16 km had been chosen. This configuration yields a maximum normal moveout of about 0.35 s for a reflecting interface at 30 km depth which might be a solid base for deriving crustal velocities from stacking velocity analyses. However, a serious problem arises from the dominance of strong diffraction patterns and the weakness and discontinuity of reflections. For this reason the preliminary stacking velocities might often be too high. Special efforts had to be made in order to solve the velocity problem.

In a restricted part of the DEKORP 2-S profile velocity functions can be derived from in-line wide-angle observations. The procedure and the results are given in Sect. 4.2.

In addition, diffraction patterns in the lower crust have been analyzed with respect to their velocity information. In a first attempt, a section of 32 km length north of the Ries astrobleme was selected, where one of the strongest diffraction clusters has been observed. The various apices of the diffraction curves in 83 consecutive shotpoint gathers were determined with the help of maximum convexity master curves. The mean effective velocities $\tilde{v}$ (from the surface to the apex) have been determined neglecting refraction effects. Master curves for discrete center-values of 5.0, 5.5, 6.0 and 6.4 km/s were used for the analysis. A better resolution than ± 0.25 km/s was not feasible by eye-inspection. Possible off-line locations of the diffraction sources have not been taken into account in this evaluation. The spatial position of some of these diffractors was investigated by a different approach (Sect. 4.1).

Figure 18 shows a diagram of the selected section where the position of the specific apices and the related values of the mean effective velocity $\tilde{v}$ are plotted in a TWT versus distance diagram. The individual $\tilde{v}$-values are denoted by different symbols. Reflection elements are indicated by up-

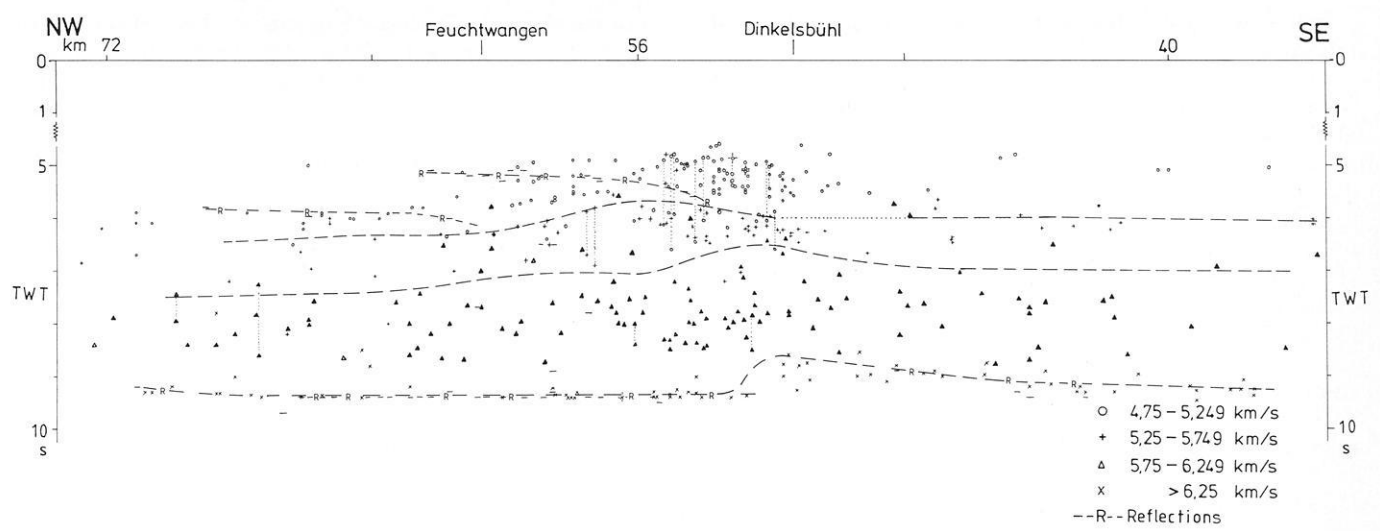

Fig. 18. Time distance diagram of apex positions and mean effective velocities picked from 83 shotpoint gathers. For further explanation see text

percase "R" and narrowly dashed lines. The dotted vertical lines indicate a corresponding arrangement of apices which could not be resolved in more detail. The clustering of apices with $\tilde{v}$-values of 5.0 ± 0.25 km/s in the center of the figure (near Dinkelsbühl) is remarkable (see the unmigrated section in Fig. 21). In a next step areas of apices with the same $\tilde{v}$-value were separated from each other by widely dashed lines. In the time range from about 5–6 s TWT surprisingly low $\tilde{v}$-values appear (4.75–5.25 km/s) except for very few singular apices related to higher velocities (5.25–5.75 km/s). One possible explanation of these low mean effective velocities is a lateral offset of the diffractors; another one is the presence of rocks with rather low velocities.

In deeper regions, especially in the Moho range, relatively high $\tilde{v}$-values are obtained. These surprising results might be caused by edge-diffractors: crossing them by profiles under oblique angles generates diffraction hyperbolas yielding higher apparent velocities than the true average velocity ($v_{\text{apparent}} = v_{\text{true}}/\sin\varphi$, where φ is the angle between profile direction and the edge-diffractor).

A more detailed processing of the profile concerning, among others, the velocity problem is under way at the DPC. Also tests using other processes than the conventional stacking method are being performed. In addition, a tomography analysis of the large first-arrival data set has been started.

3. Presentation of first seismic results and preliminary geological interpretation

3.1 Description of seismic results

Figure 19 gives an example of a typical common shotpoint gather observed along DEKORP 2-S, with 200 traces at a location near Dinkelsbühl (shotpoint 641.5). The first 12 seconds two-way traveltime (TWT) (out of 20 s recorded) are shown:

- In the upper 6 s TWT reflections are very poor or absent.
- There are several good reflections between 6 and 10 s TWT.

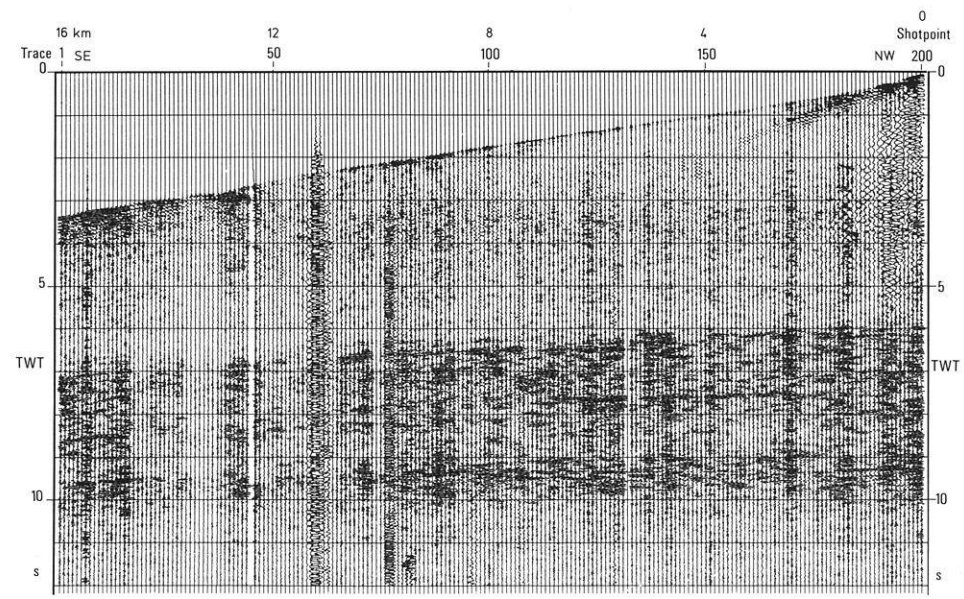

Fig. 19. Example of a DEKORP 2-S seismogram (common shotpoint gather from SP 641.5), unfiltered. Scaling function is $K \cdot T^n \cdot e^{aT}$ with $K = 1.0$, $n = 1.0$, $a = 1.1\ \text{s}^{-1}$ for $0.0\ \text{s} \leqq T \leqq 3.5\ s$ *and* $K = 164.5$, $n = 0.0$, $a = 0.0\ \text{s}^{-1}$ for $3.5\ \text{s} \leqq T \leqq 12.0\ s$ *(see Sect. 2.1)*

– Below 10 s TWT the seismic traces are again void of reflections.

The common shotpoint gather of Fig. 19 is typical in so far as generally – with a few exceptions – the early parts of the seismograms contain little information. The TWT at which a considerable increase of reflection density and quality is observed, changes along the profile coming close to only 2 s in the Spessart area. Nearly on all seismograms a strong reflection-energy band is observed between 9 and 10 s TWT which represents the last pronounced event. This event comes from the zone of the Mohorovičić discontinuity (Sect. 3.2).

The first arrivals are clearly defined along the 16 km-spread. They have been picked for all shotpoint gathers, and the information is being analyzed in order to obtain the velocity distribution in the uppermost crust.

Figure 20 shows the CMP-stacked record section of DEKORP 2-S unmigrated and uninterpreted. Figure 21 presents the same stack with some interpretation. The dominant tectonic units, a stratigraphic division and the position of major topographic units and localities are marked on the top of the figures.

The general picture of the section is dominated by numerous strong diffractions, rarely seen with such a density and strength in crustal sections. The diffractions concentrate between 5 and 10 s TWT, i.e. in the time range of the highly reflective lower crust. In the northern part of the Franconian Platform and below the Spessart, however, they ascend up to 2 s TWT. Some of these diffractions cluster strongly near the area of Dinkelsbühl (km 40–70) and below the Spessart between the Main river and the town of Laufach (km 150–190). A weaker concentration is observed between the Tauber river and Würzburg (km 110–140), and an oblique SE dipping alignment of diffractions occurs between Rothenburg and the Tauber river (km 65–110).

Picking of continuous seismic reflections is not possible over longer distances. Even the Moho band appears in the form of rather short reflecting elements. At certain locations there are pronounced dipping events, not only in the reflective lower crust but also in the upper crust, sometimes approaching the surface, such as in the Spessart and Tauber area and near Dinkelsbühl.

Dips to the southeast dominate. Some alignments of diffraction apices occur which seem to dip towards the southeast although vertically arranged clusters, such as that below Dinkelsbühl, are also observed. Most of the reflections in the DEKORP 2-S section are subhorizontal. With their clustering in the lower crust they fit well into the general picture of reflectivity from records in the Variscan belt, showing a highly reflective lower crust embedded between a poorly reflective upper crust and upper mantle (Meissner et al., 1984).

Several locations along the profile show poor quality reflections. In the Ries area such a decrease of quality may be related to lateral variations in velocity and wave-scattering caused by the brecciated basement. The reflectivity of the lower crust below the Ries seems to be similar to that in its vicinity, as indicated by the short E-W reflection profile through the Ries crater described by Angenheister and Pohl (1969, 1976).

BEB[1] provided the first migration of the entire profile (Fig. 22). Another one was processed at the DEKORP Processing Center at Clausthal later on (see Fig. 23 and Sect. 2.3) where higher velocities in the time range 0–6 s TWT have been used. The result differs in so far as some reflection events have become more pronounced so that a clearer overall picture has been obtained in Fig. 23. However, this effect might be due to slightly different parameters (e.g. scaling function or filter limits) in the processing sequence which was essentially the same for both migrations. The interpretation is based on both results.

The migrated sections contain still some curved events which could partly correspond to curved reflectors or to residual diffraction patterns. The latter ones could have been generated by edge diffractors. Some "overmigrated" events (i.e. too high migration velocity for this particular diffraction) can be produced by point diffractors at positions not vertical below the profile. The maximum spatial extent of all point diffractors has been estimated by the Fresnel zone formula to a diameter of 4.9 km at a depth of 30 km for a frequency of 15 Hz and a velocity of 6 km/s. At a depth of 15 km the diameter decreases to 3.5 km.

South of Rothenburg remarkable southeast dipping reflecting elements at the Moho level are observed which seem to originate from the sub-horizontal Moho zone. Pronounced, relatively shallow, southeast dipping events are seen below the Spessart. Generally speaking the majority of reflection elements is accumulated in the region of 50–200 km of the section with the densest concentration in the regions of the diffraction clusters of the unmigrated section. From the Spessart mountains in the north to the Ries in the South the top of the crustal reflection zone descends from 1.5 s to 5 s.

Based on the migrated sections a line-drawing, containing the most reliable reflections, is presented in Fig. 24. The positions of the apices of the most prominent diffractions taken from the unmigrated section have been added. The southeast dipping reflectors below the Spessart are clearly defined. Their dip decreases at about 5 to 6 s TWT, but there are again strongly dipping events in the lower crust below Rothenburg. In the upper crust a zone of increased reflectivity is seen northwest of Würzburg.

3.2 Depth and structure of the Moho

Reflections have been observed along DEKORP-profile 2-S down to a TWT between 8.5 and 9.5 s. Below the corresponding depth only very rare seismic events have been

[1] BEB Brigitta and Elwerath Betriebsführungsgesellschaft mbH, Hannover

Fig. 20. Uninterpreted and unmigrated stack of DEKORP 2-S. Vertical exaggeration approximately 1.5:1. Mean coverage about 22 fold. Processing parameters: predictive deconvolution with 188 ms operator length and 4 windows from 3,000–12,000 ms, AGC window: 1,000 ms. Plot parameters: 2 fold vertical stack, 12 Hz (24 dB/oct) – 45 Hz (42 dB/oct) filter, AGC window: 400 ms. Note that diffraction hyperbolas are the dominating events

Fig. 21. Unmigrated stack of DEKORP 2-S with some interpretation. Parameters as explained in caption of Fig. 20

NW SE

RHENOHERC. | SAXOTHURINGIAN | MOLDANUBIAN

Devonian | Tertiary | Crystalline Basement | Bunter | Muschelkalk | Keuper | Impact Breccia | Malm

TAUNUS | WETTERAU | SPESSART | FRANCONIAN PLATFORM | RIES | SWAB. ALB

Friedberg Hanau Laufach Main Würzburg Tauber Rothenburg Dinkelsbühl Nördlingen Donauwörth

km 250 200 150 100 50 0 km

0 5 10 s (TWT) 15

20

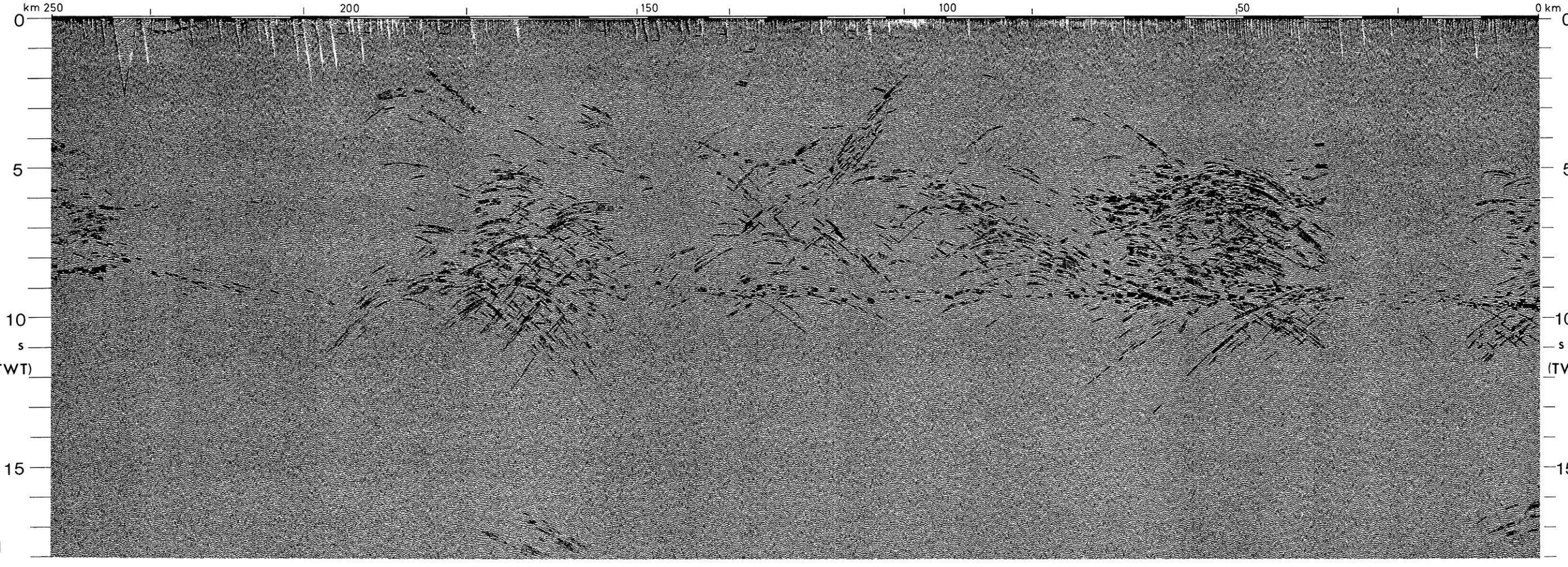

21

NW

SE

RHENOHERC. | SAXOTHURINGIAN | MOLDANUBIAN

Devonian | Tertiary | Crystalline Basement | Bunter | Muschelkalk | Keuper | Impact Breccia | Malm

TAUNUS | WETTERAU | SPESSART | FRANCONIAN PLATFORM | RIES | SWAB. ALB

Friedberg — Hanau — Laufach — Main — Würzburg — Tauber — Rothenburg — Dinkelsbühl — Nördlingen — Donauwörth

km 250 — 200 — 150 — 100 — 50 — 0 km

0 — 5 — 10 s (TWT)

22

RHENOHERC. | SAXOTHURINGIAN | MOLDANUBIAN

Devonian | Tertiary | Crystalline Basement | Bunter | Muschelkalk | Keuper | Impact Breccia | Malm

TAUNUS | WETTERAU | SPESSART | FRANCONIAN PLATFORM | RIES | SWAB. ALB

Friedberg — Hanau — Laufach — Main — Würzburg — Tauber — Rothenburg — Dinkelsbühl — Nördlingen — Donauwörth

km 250 — 200 — 150 — 100 — 50 — 0 km

0 — 5 — 10 s (TWT)

23 15

recorded. The reflections between 8.5 and 9.5 s TWT are not continuous, but a band of reflections can be defined which can be followed all along the profile with some interruptions. Converting to depth with an approximate average velocity of 6,100 m/s (see Sect. 4.3 and Bartelsen et al., 1982; Meissner et al., 1982), this band of reflections corresponds to a discontinuity zone at 26–29 km depth. Regarding the information about the depth of the Moho-discontinuity from the most recent publications (Mostaanpour, 1984; Gajewski and Prodehl, 1985), depths of 26 (near the Taunus) up to more than 28 km in the area of Nördlingen are given for locations closest to the profile.

It is intended to carry out much more detailed velocity studies from the reflection data. Only with more reliable velocity data at hand, one should discuss the question whether there is a discrepancy between the Moho as determined from reflection and refraction data, respectively, and whether this is due to anisotropy or other reasons. At this stage, we state that the somewhat discontinuous band of reflections at 8.5–9.5 s TWT at the base of the reflective crust can be considered as the Moho zone, and that there is no prominent anisotropy effect.

On the DEKORP 2-S profile the Moho below the Ries astrobleme seems to exhibit a weakly anticlinal structure. The updoming effect would still be reinforced if the correct velocities obtained from the more detailed analysis would be lower than those used so far. Such effects have not been observed in the earlier E-W profile through the western rim of the Ries (Angenheister and Pohl, 1969). Thus, no safe conclusions can be drawn at this stage.

The Moho band reveals some tectonic structure in the Dinkelsbühl area; this is shown in more detail in Sect. 4.2 where the diffraction data of that area are discussed. At the NW end of the DEKORP 2-S profile the Moho band is faulted with the upthrown side below the Taunus. The overall geotectonic situation can be solved only after the extension of profile 2 to the north.

3.3 Attempt of tectonic interpretation

It is evident that there is more information from reflected energy in the central part of the profile, approximately between Dinkelsbühl (km 50) and Hanau (km 210), than at both ends. As this part is the general area of the Saxothuringian (ST) zone, this might be the seismic expression of the different types of crustal structure in the Rhenohercynian (RH), ST and Moldanubian (MN) zones of the Variscan belt as described in Sect. 1.3. The higher reflectivity of the central section might have its cause in the remnants of highly active horizontal tectonics with crustal shortening in the ST zone. The upper crust in the Dinkelsbühl area is nearly void of any reflections, thus the suture zone between ST and MN might be dipping SE, and there is no contradiction between the MN-gneisses drilled and the seismic character of the lower crust in the same area (see Fig. 3). With the clustering of reflections in the lower crust the DEKORP 2-S section fits well in the general picture of reflectivity in the Variscan system showing a highly reflective lower crust embedded between the poorly reflective upper crust and upper mantle (Meissner et al., 1984).

In the northernmost part of the ST zone, a narrow belt of lowgrade rocks is exposed in the southern Taunus. This "Northern Phyllite Zone" is a zone of intense tectonic imbrication and polyphase deformation (Weber and Behr, 1983; Weber 1984). Since phyllitic rocks occur as tectonic shavings at the base of greywacke nappes in the RH, the Phyllite Zone is regarded as the root zone of these nappes. This implies a distance of transport of at least 60 km. At the junction of RH and ST zones (Behr, 1978; Weber and Behr, 1983) the Mid-German Crystalline High (MGCH) overrides the Phyllite zone, and both are thrust northward over the lower-grade rocks of the RH zone proper.

At the southern border of the ST a similar geological situation is encountered, where at an analogous position of the tectonic framework in the western Bohemian Massif supracrustal nappe piles were generated and transported to the northwest (e.g. the Münchberg nappes). The predominance of higher-grade metamorphic rocks in the overriding units is an expression of the same principle of metamorphic and stratigraphic inversion, which is also inferred for the intracrustal thrust-sheets that contain granulites, ecologites, garnet-peridotites and serpentinites. These phenomena could probably also be explained if one regards the overriding units at the margins as small-size crustal elements (microcontinents or exotic terranes, see, e.g. Ziegler, 1982) which during the process of collision underwent a high degree of tectonic-metamorphic reactivation, so that their margins are transitional between an intracontinental suture and a nappe-thrust.

Principally in all Mid-European pre-Permian crystalline regions the following steps of development can be observed:

- A medium-pressure/high-temperature metamorphic event (granulites, eclogites with integrated tectonic slices of high-pressure rocks).
- A subsequent mylonitization, shearing and intracrustal thrust tectonics with ductile and brittle deformation affecting the entire basement. This type of deformation is penetrative and can be observed on a regional scale. The corresponding structures in the ST are known since the beginning of this century and were studied and described in connection with the Variscan nappe tectonics. Recently, similar structures were recognized in the Black Forest and at the western border of the Bohemian Massif. Interpretation of their structural evolution is supported by numerous microtectonic studies (Behr, 1978, 1983). They comprise thrust sheets and large-scale antiforms of granulites with lateral extensions exceeding 50 km which later pierced through the overlying rocks (e.g. "Granulitgebirge"). They also include huge "horses" (phacoids), thrust slices, refolded simplex-

Fig. 22. Migrated stack of DEKORP 2-S by use of wave equation migration (type: finite difference, 52 ms interval). Parameters as explained in caption of Fig. 20. Migrated and plotted by BEB Brigitta und Elwerath Betriebsführungsgesellschaft mbH, Hannover

Fig. 23. Migrated stack of DEKORP 2-S processed by DEKORP Processing Center, Clausthal, and plotted by BEB Brigitta Elwerath Betriebsführungsgesellschaft mbH, Hannover. Processing parameters: before FD-migration bandpass filtering as given in Fig. 12 and additional 30–45 Hz antialiasing high-cut filter; after FD-migration random scaling with 1,000 ms window and 500 ms shift; bandpass filtering with 5–10 Hz low-cut and 20–35 Hz high-cut. Plot parameters as explained in caption of Fig. 20

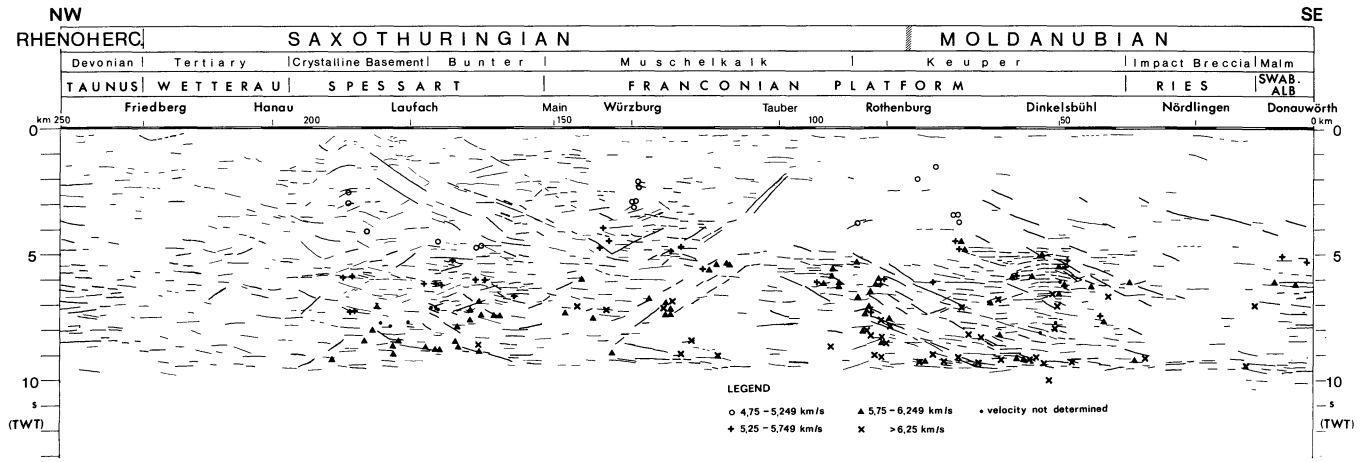

Fig. 24. Line drawing of good and strong reflections picked from the migrated sections in Figs. 22 and 23. The symbols indicate the position of apices of diffraction hyperbolas and estimated mean effective velocities obtained from analysis of the stacked section in Fig. 20 with the aid of maximum convexity master curves. Vertical exaggeration 1.5:1

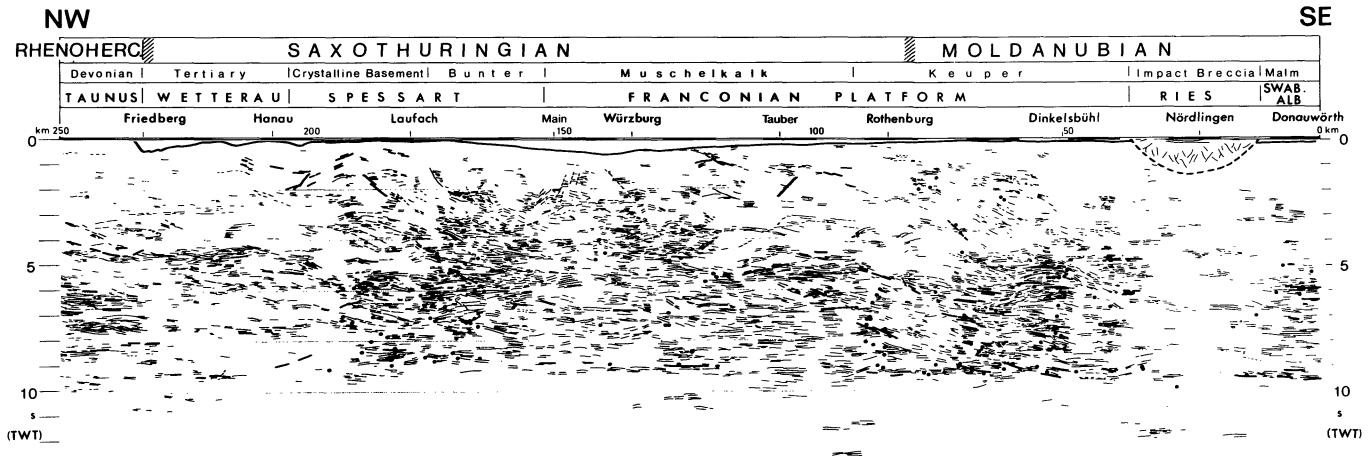

Fig. 25. Line drawing of profile DEKORP 2-S derived from the migrated section which contains all recognizable reflections including also questionable ones. Thick lines indicate high quality reflections; points are apparent diffraction apices as determined from the unmigrated stack with the aid of master curves. The continuous line below datum represents the base of the Permian derived from seismic and drilling results. The dashed line below the Ries outlines the brecciated basement. Vertical exaggeration 1.5:1

and duplex-structures, blastomylonitic belts and zones of cataclasites at various scales down to the microscopic.

– Finally, there follows a high-temperature metamorphic event producing migmatite gneisses and granitoides or partially overprinting most earlier deformation structures by recrystallization or blastesis.

The following preliminary interpretation is based on all the geophysical and geological information presented above. In order to provide more detail than in Fig. 24 it has been tried as an intermediate step in Fig. 25 to include also a large number of short and weak reflection elements; many of them might be questionable. The result of the geological interpretation is shown in Fig. 26.

At the northern border of the ST a large accretionary wedge-type interface between ST and RH is expected (Weber and Behr, 1983). First indications of high-pressure (10–12 kbar) relics in the Northern Phyllites (Masonne and Schreyer, 1983) make probable a situation like the one shown in our interpretation. The assumed depth extension of RH and Northern Phyllite Zone metasediments definitely needs further testing by detailed velocity analyses. We further assume that out of the suture zone a decollement developed toward north that was initially tied to the base of the weakly metamorphic RH. Out of this horizon numerous listric shears formed that correspond to reverse faults at the surface.

The RH zone seems to be distinguished by its originally at least 6–8 km thick metasedimentary cover overlying a rheologically distinctly different basement. This, we suppose, renders it likely that the displacement was largely transferred by a single thrust zone at the base of the suprastructure. It would imply less structural perturbation in the RH basement and thus more persistent subhorizontal reflections could be expected north of the RH/ST suture.

At the border ST/MN the situation is different. Here, two polymetamorphic crustal segments collided. In contrast to the northern border, the shear zone dips steeper and causes stronger rotations and more intensive interstacking, starting in the basement and continuing into the suprastructure. Therefore, particularly in the southern part of the

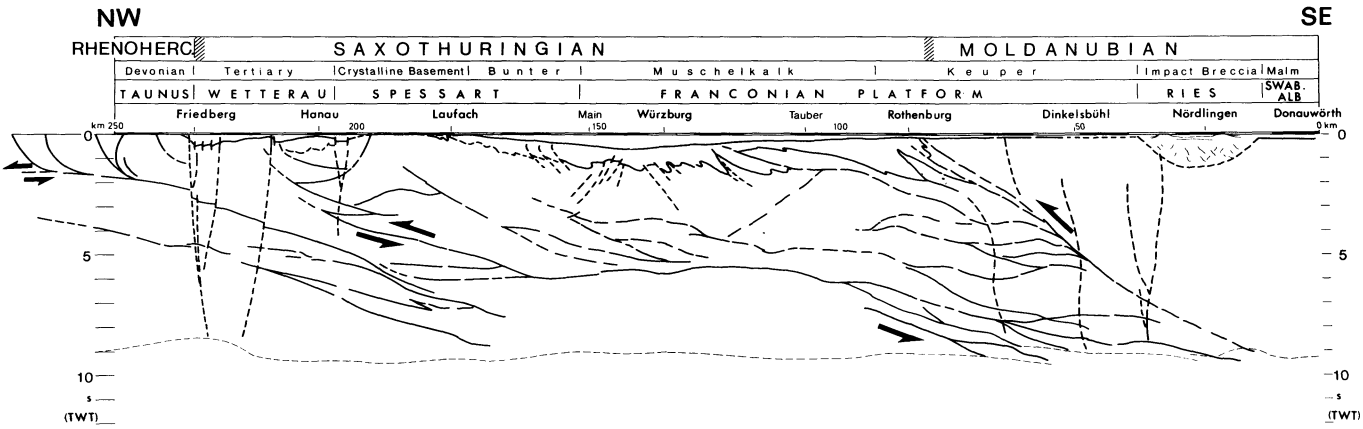

Fig. 26. Preliminary structural model along profile DEKORP 2-S based on a thrust concept. The first line below the datum shows the base of the Permian. Dashed lines indicate hypothetical downward extensions of post-Permian normal faults. For further explanation see text. Vertical exaggeration 1.5:1

border zone isolated fragments from the lower crust and upper mantle were transferred even into the top of the upper crust. This is also supported by the southeast dipping strong reflections reaching down to the Moho in the Rothenburg-Dinkelsbühl area. An equivalent situation is known at this border zone in the Bohemian Massif (Behr et al., 1984).

The assumption of a thrust-body below the Tauber is only vaguely supported by the seismic data. There are only some short reflections. But there are strong magnetic and gravity highs in the Tauber area (Figs. 4 and 5 in Sect. 1.3). This hypothetical structure may be regarded as an analogue to the "Münchberger Gneissmasse" situated in an equivalent tectonic position farther east.

With regard to the basement depth of the ST sedimentary cover, no information can be retrieved from the seismic section. It was assumed on the basis of general knowledge about the structural style and approximate thickness of the ST suprastructure.

The optimal estimation of exact interval velocities in combination with gravity model calculations could help to decide whether the crust was doubled along the south dipping structures on a large scale. However, there exists certainly a large system of thrusts between the northern and southern border of the ST. This is indicated by reflection structures as well as by the arrangements of diffraction apices along SE dipping lines, e.g. below Rothenburg and the Spessart (Fig. 24 and 25). The middle portion of the shear zone seems to parallel the top of the lower crust. At its northern extremity it should accomodate considerable displacement. For instance, the crystalline Spessart should have been uplifted along those shears from the level of 4–5 kbar (Matthes, 1954).

Regarding the southern part of the shear system there should be a direct connection to the Moho. This might also be indicated by the diffraction and reflection elements in single seismograms recorded in the area north of the Ries astrobleme (see Fig. 18 and Sect. 2.5). The seismic picture below Dinkelsbühl and the Spessart may be explained by the deformation processes that have been active at the ramps of this thrust system.

Ductile shears next to brittle deformation may develop due to:
- differences in viscosity due to strong composition contrasts, e.g. ultramafic next to felsic,
- dry next to H_2O-rich compositions,
- inhomogeneous migration of fluids as well as fluid controlled heat transfer,
- melting due to pressure decrease during uplift,
- mineral reactions entailing volume changes and dehydration.

Crustal domains showing strong inhomogeneities with respect to the above parameters will, therefore, tend to develop into an aggregate of sheared bodies of limited extension (e.g. huge horses). Map patterns from the neighbouring basement outcrops of the western Bohemian Massif and the Black Forest reflect such complex situations. The exposed basement appears as a complex puzzle of lithologically diverse tectonically laminated units displaying arcuate patterns of planar and linear fabric elements with mylonites and cataclasites intervening where attitudes of layering and foliation change abruptly.

It has been tried also to derive a fracture pattern which attempts to explain Variscan basin formation and deformation purely by normal faulting (Fig. 27). Though we believe that the ST basin was initiated by crustal stretching and rifting, we also know from surface geology that subsequent deformation led to considerable crustal shortening. Some of the preexisting, probably listric, extensional faults may have been reactivated with opposite shear sense during the latter event. However, the hypothetic fracture pattern as shown in Fig. 27 can by no means accomodate the shortening necessary to bring for example eclogites into the suprastructure as exposed in the Münchberger Massif which represents an analogous tectonic position. In domains of high pore pressures and concomitant low effective shear stresses extensional faults and veins may form locally even in shear zones where ductile rheology changes into a brittle one. In this way diffraction points and edges (Fig. 24) may also be explained.

The late- and post-Variscan development led to the subsidence of Permian and Tertiary basins through extensional faulting. This may explain slight crustal thinning and Moho steps. The apparent arrangement in a near-vertical pattern and in the strike direction of the Variscides and the concentration of diffracting elements in the lower crust below Dinkelsbühl (Fig. 21 and 24) may point to magmatic intrusions along such vertical extensional features, too. We consider this a possible alternative cause for the Dinkelsbühl and

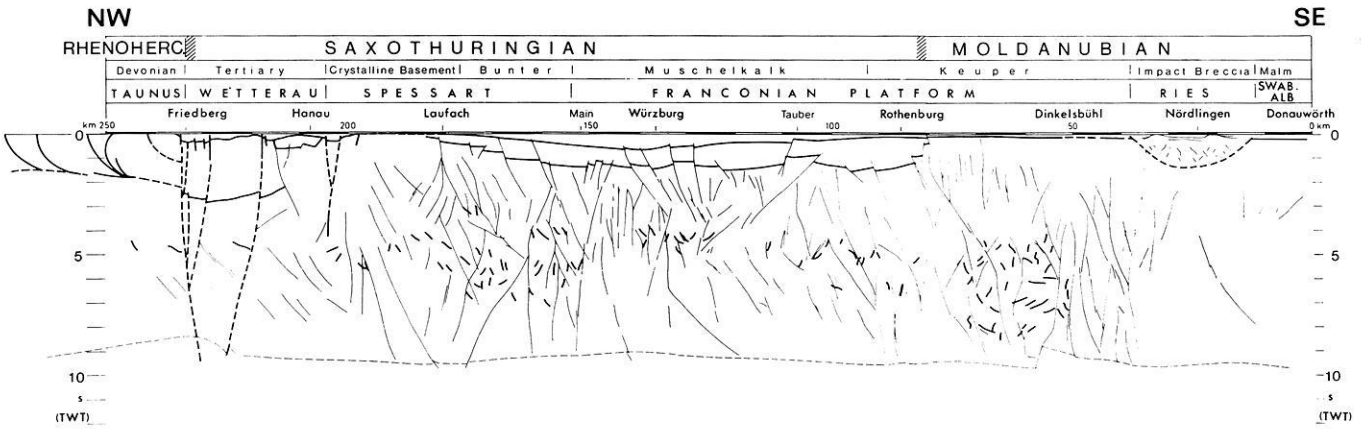

Fig. 27. Alternative structural model based on extensional tectonics concept. For further explanation see text. Vertical exaggeration: 1.5:1

Spessart diffraction clusters, though Permian and younger basins are missing from the above areas. The fault pattern north of the Spessart results from an analysis of surface geologic data (Wenz, 1936; Golwer, 1968) and of a shallow reflector interpreted as the top of the pre-Permian basement.

4. Accompanying seismic activities and their first results

4.1 Near-vertical observations of crews from universities and other research institutions

The objectives of the additional reflection observations on lines Q_1 and Q_2 (Fig. 2) were:
- Studying the lateral continuation of crustal reflection data in order to obtain a quasi 3-D picture in a certain area, especially the construction of parallel and perpendicular profiles and the determination of true strike and dip angles.
- Collecting data from undershooting the Ries astrobleme.

The additional reflection observations were carried out in the area north of the Ries astrobleme (line Q_1) by means of five individual digital reflection recording units[2] with a total capacity of 120 channels. Using the shots along the main profile and five additional shots west of it, a three-dimensional control of the subsurface was obtained in an area of about 200 km^2 size east of the main profile (see Fig. 28). The major part of the additional geophone groups, i.e. 108 traces, were placed perpendicular to the main profile, the other 12 groups parallel to the main line (Fig. 2). Because of the different directions between shots and geophones an areal pattern of 24 geophones with a rather constant angular characteristic was used for all 120 traces. This pattern remained fixed throughout the operation. A grid with squares of 40×40 m^2 was applied for the construction of "common midpoints" (CMP) in the area, while in Fig. 28 only the coverage by 320×320 m^2 squares is shown. Thus, a six-fold coverage was obtained on average. Amplitudes were normalized to those of the first arrivals, and no further automatic gain control (AGC) was necessary, an effect of the large offsets. A band-pass filter from 12–45 Hz was used, the dominant signal frequency being around 20 Hz.

[2] Operated by teams from Clausthal, Hamburg, Hannover and Kiel

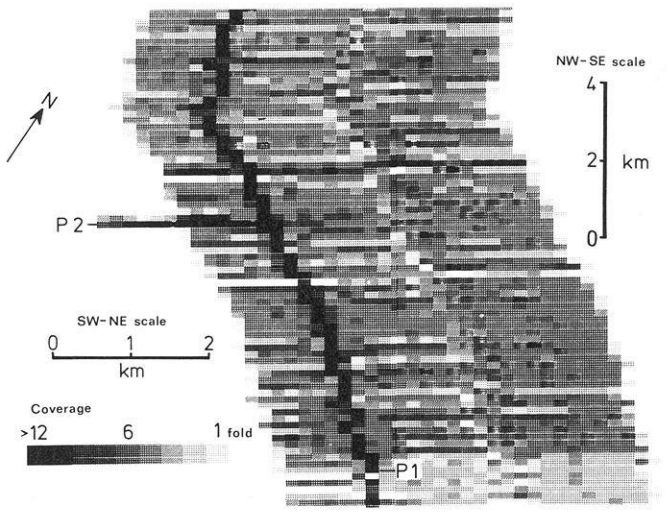

Fig. 28. Degree of coverage by 320×320 m^2 CMP squares for the additional near-angle observations of the university teams. Vertical to horizontal scale ratio is 2:1. Black squares indicating the highest degree of coverage display the position of the parallel profile P1 (see Figs 30–32)

The construction of a parallel profile P1. The 12 parallel geophone groups and the shotpoints along the main profile were used as a basis for the construction of the first parallel profile P1, parallel with DEKORP 2-S (see also Fig. 29). It starts in the center of the Ries astrobleme, at about km 20 of the main profile, and ends at km 72 in the north. Two consecutive traces were interpolated and plotted at the common midpoints along the line. The maximum offset-difference for stacking was 3 km. Stacking velocities from refraction data in the vicinity and from reflection data along the Urach profiles (Bartelsen et al., 1982; Meissner et al., 1982) were used. Special corrections were applied for the area of the Ries astrobleme in order to take account of the near-surface low-velocity-layers.

The stacked seismogram section of P1 is shown in Fig. 30, while Fig. 31 shows a line drawing of the major reflections (solid lines) and diffractions (broken lines). The density of reflections and diffractions is similar to those along the main profile, and most of these events can be correlated. The reflections and the diffractions concentrate between 5.5 and 9.5 s TWT. Figure 32 shows an "energy

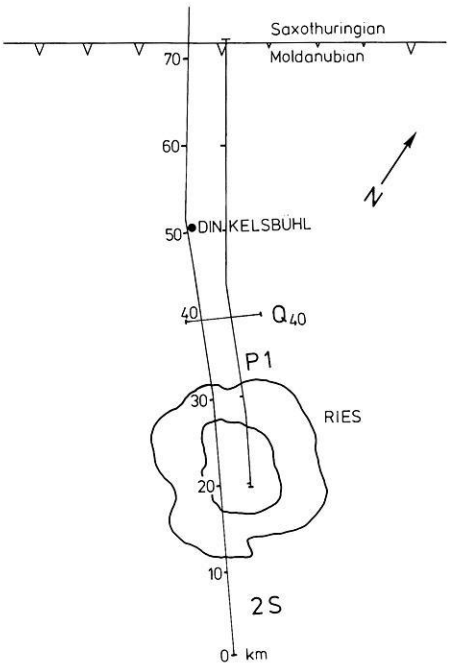

Fig. 29. Location map of the parallel profile P1 and perpendicular profile Q40

section" of P1. For this section an average of 8 consecutive traces equivalent to 320 m was formed and a moving time window of 200 ms was applied. Squared amplitudes have been normalized with regard to the maximum amplitude per trace. This energy section is dominated by the energy of diffractions which can be followed across the whole P1-section, being especially strong in the northern sector. Also in this presentation Conrad- and Moho-bands are clearly defined, sometimes also a sub-Conrad, even below the Ries astrobleme in the south. But also individual correlations of reflections from the Moho- and Conrad-bands (Fig. 31) as well as of diffractions can be made all along P1.

The perpendicular profile Q40. Profile Q40 is in the strike direction of the Variscides and is one of six perpendicular profiles constructed so far. It crosses the main profile at km 40 (as seen in Fig. 29) and makes use of 5 additional shotpoints west of the main profile and the 108 geophone groups east of it (see Q1 in Fig. 2). The 5 additional shots and 3 shots from the main profile around km 40 were used for stacking. The width of the grid was increased to 80×80 m^2.

Figure 33a presents the profile Q40 without interpretation. Its quality is slightly better than that along P1, especially reflections come out clearer than the diffraction events. Only some of these diffractions can be tied to and correlated with those along the main profile, profile P1, and the additional perpendicular profiles (not shown here). See also the line drawing section, shown in Fig. 33b. Again, reflection bands from Conrad and Moho mark the beginning and the termination of the highly reflective lower crust. Also the "energy section" (Fig. 33c) shows these two reflection bands.

On the positioning of diffraction sources. Special attention was given to the Dinkelsbühl diffraction pattern along the DEKORP 2-S profile which can also be detected along P1 (Figs. 30–32). In a first attempt, a correlation of the main

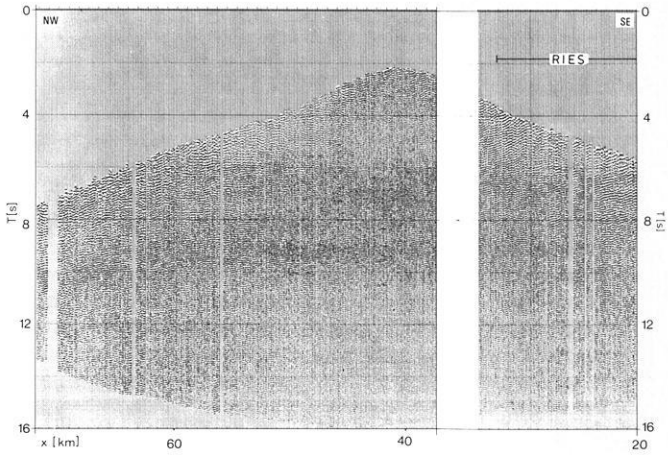

Fig. 30. Uninterpreted and unmigrated stack along the parallel profile P1. Horizontal exaggeration approximately 1.5:1. The gap is caused by technical reasons. For further explanation see text

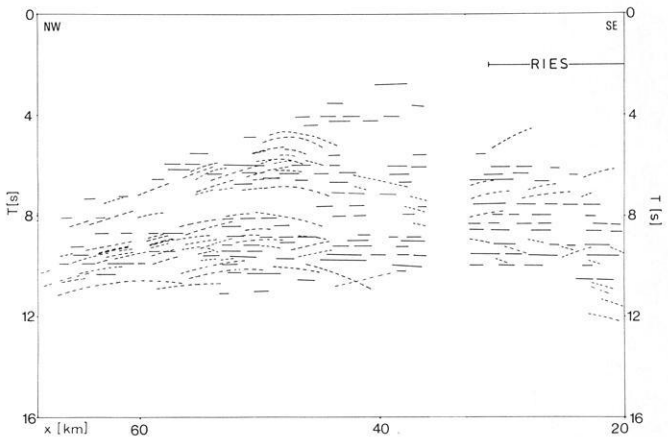

Fig. 31. Line drawing of the parallel profile P1. Horizontal exaggeration approximately 1.5:1. For further explanation see text

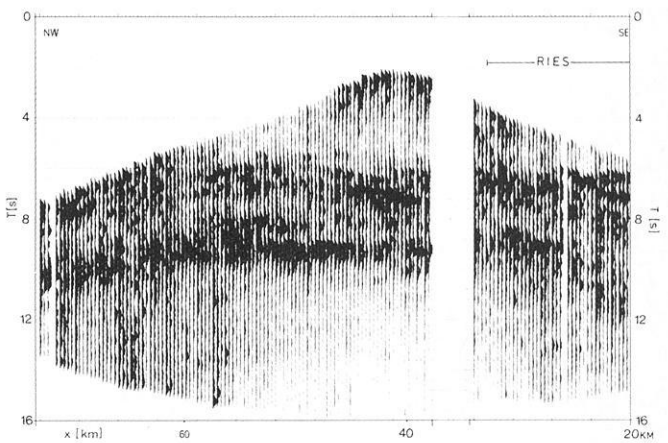

Fig. 32. Energy section along the parallel profile P1. Horizontal exaggeration approximately 1.5:1. For further explanation see text

events from DEKORP 2-S to Q40 (at km 40) and again to P1 was tried, but only bands from prominent diffractions or reflections like those of the Conrad and Moho, not single phases, could be successfully correlated around the three lines. Some of the Dinkelsbühl diffractions could be followed onto Q40, and here their dip could be determined. Some of them appear as horizontal events, indicating a

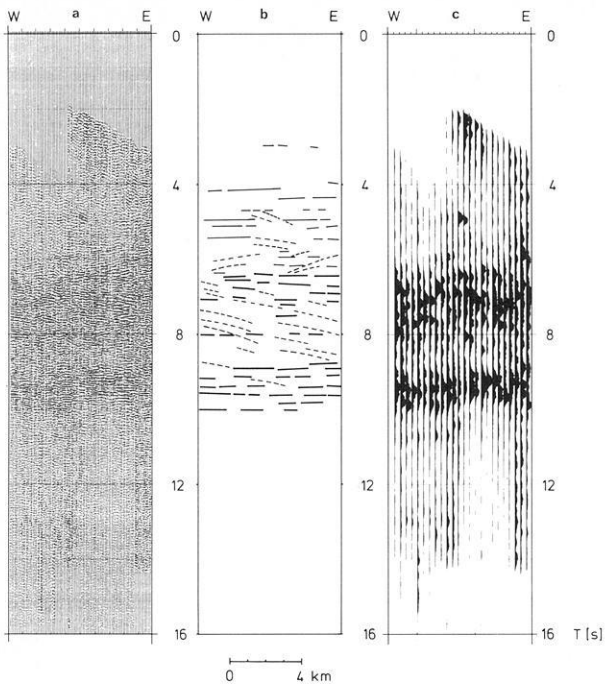

Fig. 33a–c. The perpendicular profile Q40: uninterpreted version (**a**), line drawing (**b**) and energy section (**c**). Horizontal exaggeration approximately 1.5:1

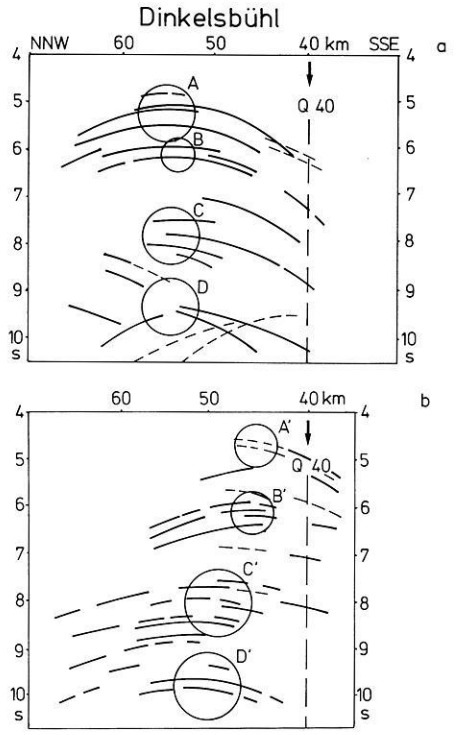

Fig. 35a, b. Significant diffraction curves with clusters indicated along DEKORP 2-S (**a**) and along P1 (**b**)

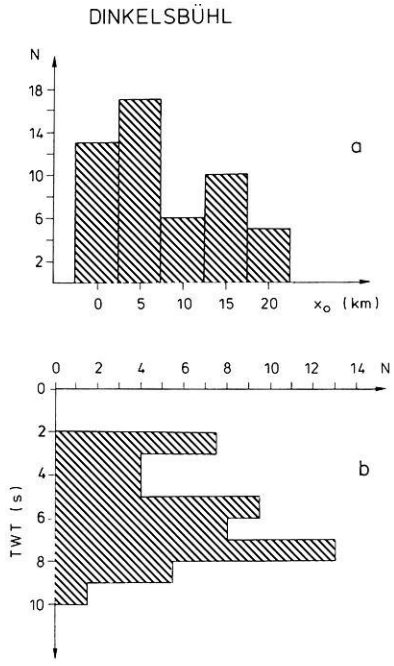

Fig. 34a, b. Distribution of lateral offsets of diffraction apices (**a**) and frequency-time distribution of corrected apices (**b**) (x_0 = lateral offset; N = number of apices)

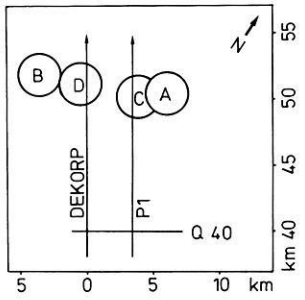

Fig. 36. Location map of diffraction clusters (A) to (D) and seismic lines

line diffractor in the Variscan strike direction parallel to Q40. The early diffractions come from sources on both sides of the main profile; the later ones show westerly components, i.e. their apices lie east of the main profile.

For a better positioning of the apices, several diffraction charts (=curves of maximum convexity) were constructed for offsets of 0, 5, 10, 15, and 20 km from the profiles. For the Dinkelsbühl diffraction cluster along DEKORP 2-S the best fit of the curvature of the events allowed to determine the offset of the individual diffractions. The E-W ambiguity could be resolved by means of the profile Q40, as mentioned above.

Figure 34 shows the distribution of the Dinkelsbühl diffraction apices as a function of lateral offsets and of TWT. Apices in Fig. 34b are corrected for lateral offsets. The peaks of the distribution resemble those of the Conrad and Moho bands. Figure 35 presents a line drawing of the most powerful and correlatable diffractions along the DEKORP 2-S and the P1 profiles and some clusters A to D. Although no exact phase correlation could be performed, the correlation along "bands" and the similarity of diffraction clusters on the DEKORP and the P1 line definitely permit a positioning of the main clusters. Their location is shown in Fig. 36. The various aspects of the interpretation of the diffraction sources are discussed at the end of Sect. 3.3.

4.2 In-line wide-angle observations by means of the reflection spreads on the main profile

27 additional shots with charges of 90 kg were fired in-line along the main profile (km 105–148). They had a distance of 65 km from the center of the 16 km long reflection spread and were recorded by the 200 trace contractor's equipment. This test was carried out in order to obtain additional structural and velocity information by comparing the wide angle with the near vertical reflection data using the same advanced technology of recording. The average distance between these shots was 1.5 km providing a five-fold coverage of the CMP elements.

The processsing of the data presented here was performed by aid of a VAX 11/780 computer at the Federal Institute for Geosciences and Natural Resources (BGR) in Hannover. Two different methods for velocity determination were chosen. Both methods suffer from the large offset with unknown refraction effects and lateral irregularities in the velocities.

The first method makes use of the assumption of true hyperbolas as traveltime branches extrapolated to zero offset times. The trial stacks resulted in a broad scatter of calculated velocity values, and only an average and two extreme velocity-time functions can be given (see Fig. 37, lines a, b and c).

In the second method trial stacks were related to an offset of 65 km. Straight lines and hyperbolas were used for the stacking of the data, and a uniform reduction of these stacks to the zero offset t_0-time was performed as indicated by line d in Fig. 37.

As a next step four trial zero-offset stacks according to the four velocity functions a, b, c and d in Fig. 37 were made. Surprisingly the best results were obtained by using curve c, i.e. the high velocity extreme of the first method. The value of the used stacking velocity at 9.5 s TWT (i.e.

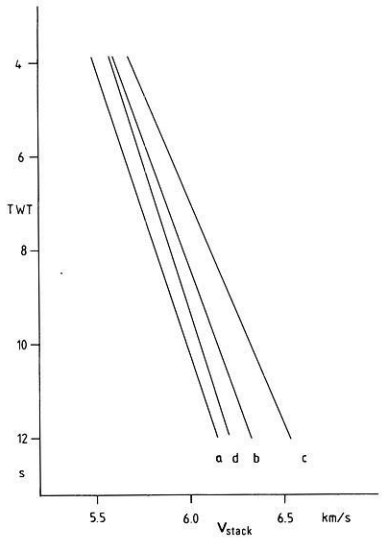

Fig. 37. Stacking velocity functions obtained from the evaluation of the in-line wide-angle observations. For further explanation see text

the Moho range) is 6.25 km/s which seems to coincide roughly with the values given in Sect. 4.3. The resulting stacked section using velocity function "c" is shown in Fig. 38. It has a 2.5:1 ratio of the horizontal to the vertical scale. Many features of the near-vertical sections (see Figs. 20–23) can be observed in the wide-angle section, too: the beginning of the highly reflective lower crust at 6 s TWT (especially in the southern part) and its termination at the Moho at about 9.5 s TWT. In the central part of the section a group of southeast dipping reflections at 7.5–8.5 s TWT is observed similar to those in the near-vertical section which shows diffractions in this region (Fig. 21). The zones of poor reflection quality are similar in both sections. Even

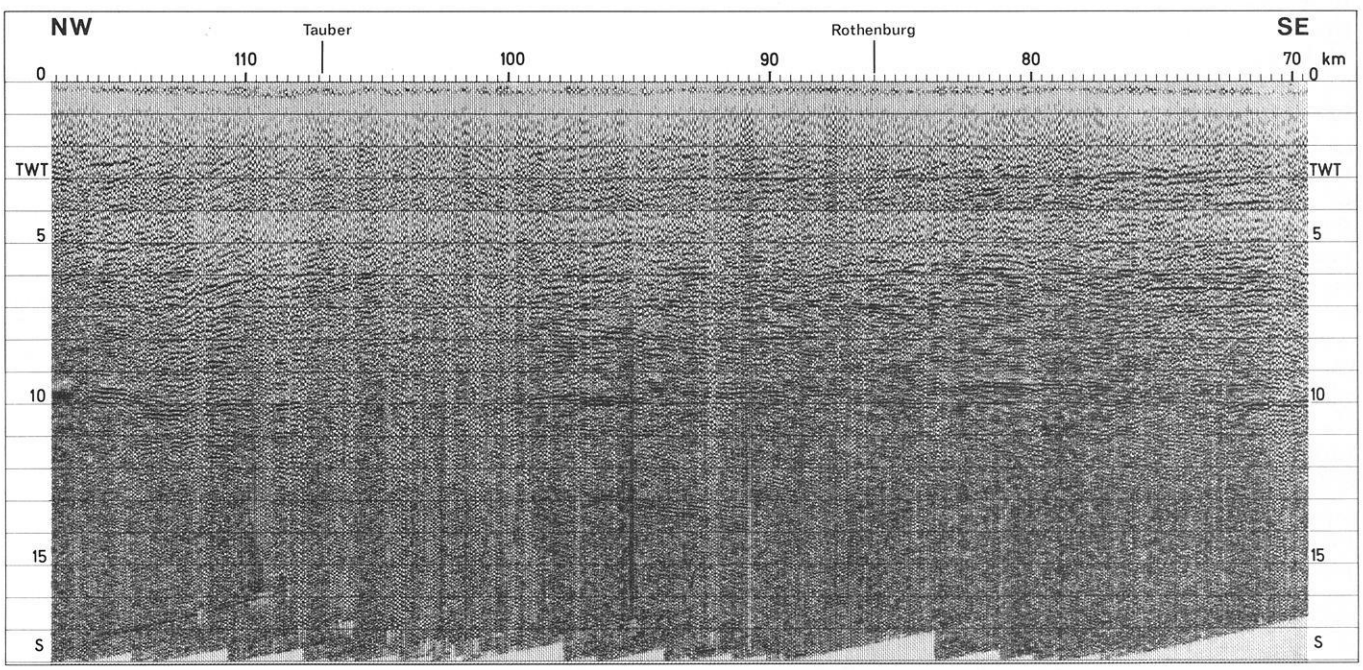

Fig. 38. Stack of the in-line wide-angle data by use of velocity function c (see Fig. 37). 6–25 Hz bandpass filter. Mean coverage about 5 fold. Horizontal exaggeration approximately 2.5:1. For further explanation see text

the continuity of reflections with a maximum phase correlation up to 15 km is comparable. Generally, the Moho comes out clearer in wide angle than in near vertical stacks, most probably an effect of a velocity gradient zone in the range of the crust/mantle transition.

4.3 In-line and off-line wide-angle studies of universities in the southern sector

The DEKORP shots in the southern sector were used additionally for refraction and wide-angle reflection observations with arrays of 10 and 24 MARS stations (Berckhemer, 1970), respectively[3]. The 10 station array remained stationary near km 100 of the main line (see Fig. 2) and thus a multiply covered in-line refraction profile was observed with shot-receiver distances up to 100 km; a total of 3020 3-component seismograms was recorded, which could only partly be processed so far.

A specially designed wide-angle experiment was carried out by the 24 station array along a parallel line with lateral offset of 50 km from the main profile; details are shown in Fig. 39. Between April 6 and 11, while shots moved from the center of the Ries astrobleme towards the presumed boundary between Moldanubian and Saxothuringian, the mobile 24 km long MARS array moved simultaneously from the center of the wide-angle line southeast of Neustadt to the northwest keeping the mean shot-receiver distance fixed at the critical Moho-distance of about 70 km. Starting April 12 the array was deployed at the southeastern end of the wide-angle line and followed the shots with the same mean distance, both units proceeding to the northwest. At the end of the experiment the stations occupied again their starting positions.

The main goal of the experiment was the investigation of the spatial structure of the crust along a traverse as extension of the structures observed on the main profile. The velocity and depth information derivable from wide-angle observations can be attached in a first approximation to the shot-receiver midpoints. They line up midway between the shot and station profiles, i.e. 25 km northeast of the main profile. For example, recording of a shot northwest of Dinkelsbühl by a 24 km long station array northwest of Neustadt yields information beneath a 12 km long midpoint profile "CMP" as indicated in Fig. 39. The same midpoints are again covered, when the shotpoint moved to Weikersheim and the station array is located east of Ansbach; ray paths in the latter case are more or less perpendicular to the ones in the first case. This offers several advantages in velocity and depth determination, when both sets of observations are jointly evaluated. However, these advantages can be exploited only after all data have been digitized and processed, and this has not yet been accomplished. At the beginning and at the end of the experiment the 24 MARS stations observed two additional refraction profiles obliquely connecting the main near-vertical profile with the wide-angle line as shown in Fig. 2.

Due to organizational and technical reasons it was necessary to record not only the 90 kg shots, as originally planned, but also all the smaller ones. In the southern part many of the small shots gave excellent results, but with shotpoints proceeding to the northwest seismic efficiency

[3] Operated by teams from Berlin, Bochum, Clausthal, Karlsruhe, Kiel, Munich and Münster. The radio-communication was provided by the NLfB

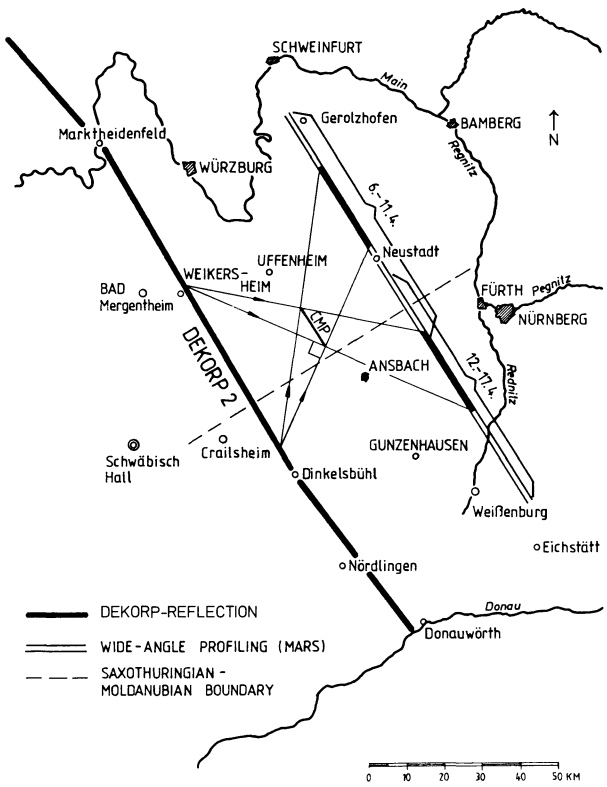

Fig. 39. Location map of the off-line wide-angle observations. The common midpoints are covered by perpendicular intersecting families of rays

became poorer. In the Muschelkalk area, where most shots had to be fired in partly dry limestone, even many 90 kg shots failed to overcome the mean ambient noise level of about 1.5×10^{-5} cm/s at wide angle distances. On the other hand, Moho reflection amplitudes up to 10^{-3} cm/s (at frequencies between 10 and 15 Hz) were obtained for many low-charge shots fired in the wet sediments filling the Ries astrobleme.

The following discussion is restricted to the external wide-angle line and is based on data from the first half of the experiment. About 50% of the 3,400 3-channel seismic records of this part of the experiment have been digitized so far. The rest was inspected but rejected from further processing due to insufficient signal to noise ratio, although within a series of less efficient shots some records of rather small signal to noise ratio have been retained for the sake of a uniform coverage. After digitizing and demultiplexing further processing was performed on a PDP 11/40 multipurpose computer of the Institut für Allgemeine und Angewandte Geophysik at the University of Munich.

Figure 40 shows a detailed location map of the stations and shots processed so far. Stations with odd numbers were equipped with 3-component seismometers and stations with even numbers had 3 vertical seismometers with a spacing of 300–400 m. On the basis of raw seismogram sections for every station poor seismograms were sorted out and the remaining 1892 vertical traces were passed through a high-cut 25 Hz-filter for further noise reduction. Dominant frequencies of most wide-angle seismograms are about 10–15 Hz.

In addition to the shotpoints and recording sites Fig. 40 shows the locations of the shot-geophone midpoints of the

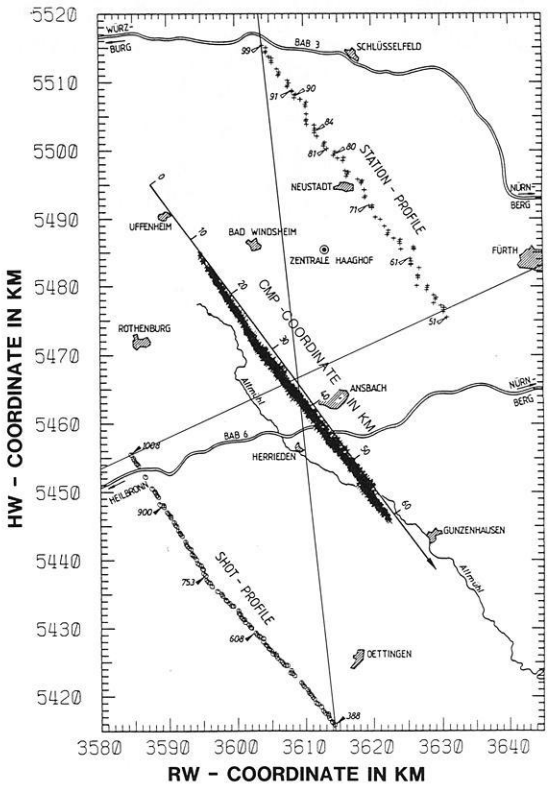

Fig. 40. Detailed location map of shotpoints, recording sites and common midpoints for the wide-angle data processed so far

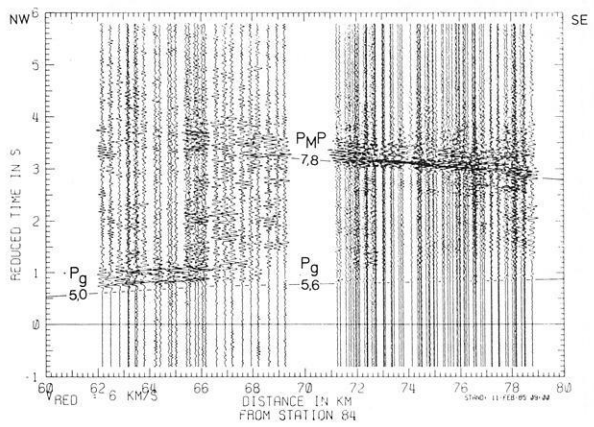

Fig. 41. Wide-angle record section for station 84 and moving shotpoints. The Moho shows up as prominent reflector; the crust looks almost transparent. Maximum amplitudes in all traces are the same; this applies also to Figs. 42–48

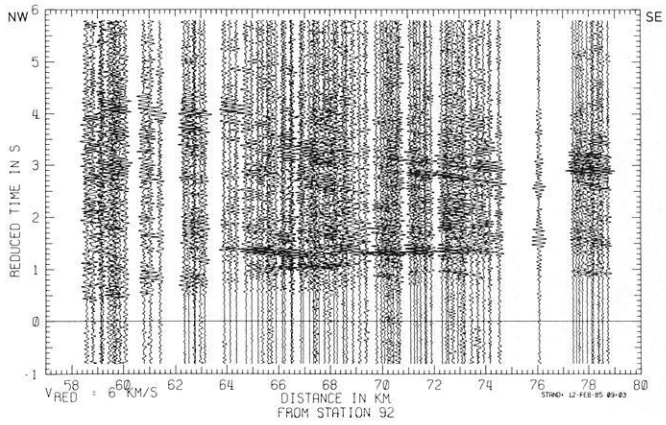

Fig. 42. Wide-angle record section for station 92, only 8 km apart from station 84 but exhibiting quite different crustal properties

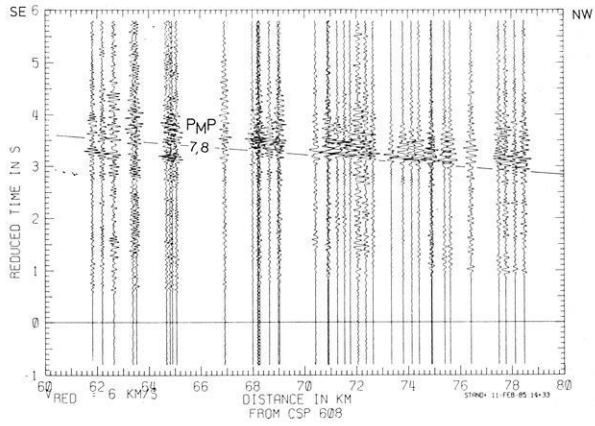

Fig. 43. Example of a common shotpoint (CSP) record section (SP 608) which is partly inverted in comparison to Fig. 41

selected vertical seismograms. Due to the multifold coverage the midpoints form an elongated black cloud. They can be described by a linear common-midpoint (CMP) coordinate, the origin of which has been fixed arbitrarily.

The large amount of data allows the construction of common-station (CST) and common-shotpoint (CSP) as well as common-offset (COF) and common-midpoint (CMP) seismogram sections. Some typical examples are shown in Figs. 41–46.

The most outstanding result is the strong crustal heterogeneity, which is reflected by the seismogram sections of adjacent shots and stations. For instance, station 84 (Fig. 41) shows clear P_g onsets and a pronounced and continuous Moho reflection (P_MP) with a reasonable apparent velocity of 7.8 km/s, but almost no correlatable signals in between. Station 92 (Fig. 42), however, located only 8 km apart gives a completely different picture with a disintegrated P_g phase, a complicated multiple Moho phase with extremely large apparent velocities and very strong intracrustal reflections of undulatory shape. Comparison of the common shotpoint sections 608 (Fig. 43) and 753 (Fig. 44) reveals similarly large differences within short distances. When more examples are studied, a trend of first decreasing and then increasing complexity is discernible with shots or stations moving from the southeast to the northwest. Short reflection segments between P_g and P_MP exhibiting very large apparent velocities on the shot sections but only moderate apparent velocities on the reversed station sections are frequently observed. This indicates the existence of generally southeast dipping reflecting elements in the middle and lower crust, in qualitative agreement with the near-vertical reflection results on the main profile. A detailed evaluation of these phenomena will require 3-dimensional modelling and extensive ray-tracing calculations and is beyond the scope of this first report.

A more direct approach can be based on common offset and common midpoint sections, as shown in Figs. 45 and

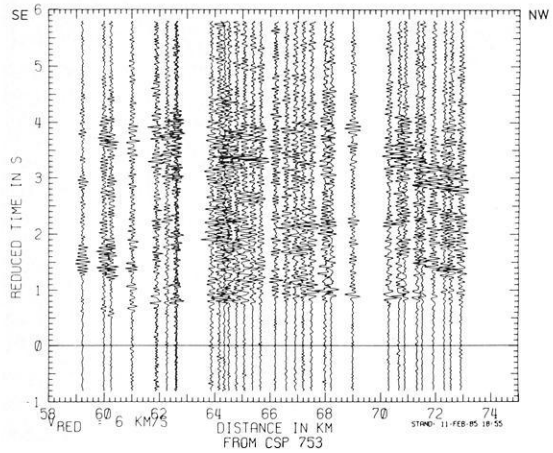

Fig. 44. Wide-angle record section for shotpoint 753, 10 km apart from shotpoint 608

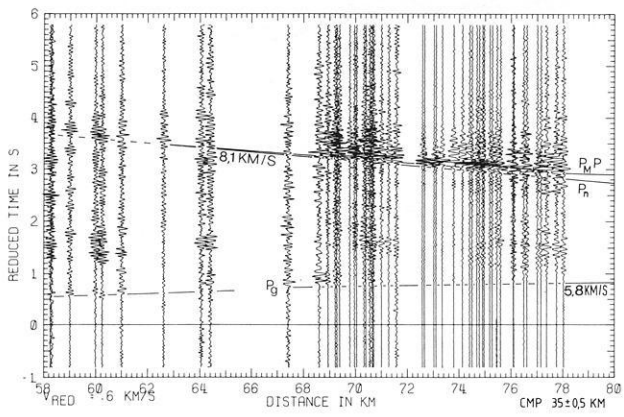

Fig. 46. Example of a common-midpoint wide-angle record section suited for velocity and depth determinations (CMP 35). This section is typical for the central part of the CMP-profile; other parts show more complexity. Distance corresponds to azimothal directions N26°E to N5°

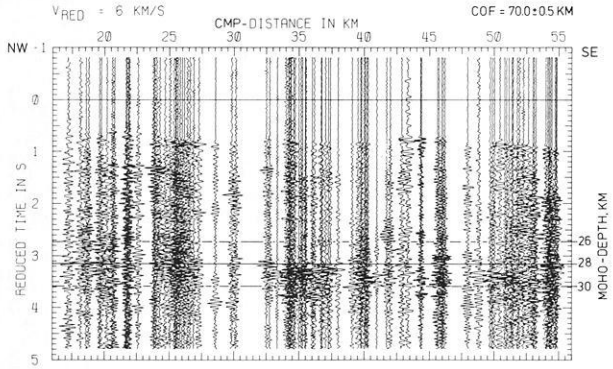

Fig. 45. Example of a common-offset wide-angle section. Offset is 70 km. Seismograms are plotted downward at the CMP-coordinate defined in Fig. 40

46. COF wide-angle sections yield a picture of crustal structure comparable to zero-offset reflection data and can be interpreted similarly. Figure 45 gives an example for an offset of 70 km. (Seismograms with shot-receiver distances within 70 ± 0.5 km have been corrected to the nominal offset according to an average apparent velocity of 7.0 km/s). For easier comparison with the near-vertical reflection data the reduced time has been plotted downward in Fig. 45; the horizontal axis is the CMP coordinate defined in Fig. 40. The Moho can be recognized at reduced times between 3.0 (CMP 30) and 3.4 s (CMP 50) and shows pronounced variations in depth, sharpness and continuity within short distances. (Such variations would hardly be detectable with classical methods of deep seismic sounding involving few shotpoints and station spacings of several kilometers.) Some southeastward dipping structures within the crust are also discernible in Fig. 45. By tuning the COF distance some of them can be imaged even more clearly.

In order to convert COF time sections into depth sections at least effective average velocities are required. They can be obtained by the analysis of CMP wide-angle sections, an example of which is shown in Fig. 46. This section contains all vertical seismograms with CMP coordinates of 35 ± 0.5 km (see Fig. 40). CMP sections focus on much smaller subsurface elements than CSP or CST sections; they are therefore less affected by lateral heterogeneities and allow some reliable velocity and depth determinations.

Since the seismic profiles have been observed perpendicular to the strike of the main geological structures and geophysical anomalies, the effective average velocity $\tilde{v}$ down to a reflector and the vertical depth z_{CMP} beneath the CMP can be calculated according to the simplified formulae:

$$\tilde{v} = \cos\alpha \sqrt{\frac{\Delta v_{\mathrm{CMP}}}{T}} \lesssim \sqrt{\frac{\Delta v_{\mathrm{CMP}}}{T}}$$

and

$$z_{\mathrm{CMP}} = \frac{\Delta}{2} \sqrt{\frac{T v_{\mathrm{CMP}}}{\Delta} - 1 - \left(\frac{D}{\Delta} \tan\alpha\right)^2} \lesssim \frac{\Delta}{2} \sqrt{\frac{T v_{\mathrm{CMP}}}{\Delta} - 1}$$

where Δ, T and v_{CMP} are distance, traveltime and apparent velocity of a wide-angle reflection in a CMP gather, α is the unknown in-line slope of the reflector and D is the normal offset between the shot and station profiles, i.e. 50 km in our case. By neglecting the weak influence of dip one obtains upper bounds for $\tilde{v}$ and z_{CMP}. (This remains true, even if additional vertical velocity variations exist.)

Applying these formulae to the data of Fig. 46 gives an average crustal velocity $\tilde{v} = 6.0$ km/s and a Moho depth of 28 km at CMP 35. If this average crustal velocity is assumed to be constant for the whole CMP line, the Moho traveltimes of Fig. 45 can be converted into Moho depths according to the depth scale indicated on the right of this figure.

Velocity determinations for other CMP gathers more to the north and to the south gave slightly higher values (6.1–6.2 km/s), but seem to be less accurate because the corresponding CMP sections are less clear than Fig. 46. In view of Fig. 45 this may not be surprising.

Attempts to resolve separate average velocities for the upper and lower crust have failed so far, because sufficiently continuous intracrustal wide-angle reflections could not yet be identified. Their shape is additionally disturbed by so far uncorrected sedimentary layers of variable thickness and velocity. It seems necessary to first correct these influences

by using all available refraction information before more details can be extracted from the CMP velocity analysis.

4.4 In-line wide-angle studies of universities in the northern sector

In-line refraction and wide-angle observations were continued between May 7 and 17 in the northern sector[4]. In addition, six automatic magnetic longtime recording stations (MLR) were in operation in the southern Spessart and in the northern Taunus. The area covered by the wide-angle observations is indicated in Fig. 2. The southernmost station was near the Main river. Nine of the southern stations along the eastern flank of the Spessart mountains were equipped with MARK 3-component geophones, the other stations used FS 60 instruments with 2 vertical and 1 horizontal component operating. The distance between stations was 540 m providing a spread length of 11 km.

During the first 8 days of operation the stations remained fixed while the shotpoints moved from the northern end of the spread towards northwest up to the critical distance of the Moho reflection. In the last two days of operation the refraction spread was moved together with the shotpoints, i.e. about 10 km per day.

At each station about 250 shots were recorded by FM technique. More than 6,000 seismograms or about 9,000 traces are available, and the digitization is not finished yet. In general, the data quality is good; even the signals from the small shots of 10 kg are clearly recognizable in the critical distance range. Only after the shotpoint had crossed the Hessian trough and moved into the Devonian of the Rhenish Massif the signals from the smaller shots could not be observed any more. The frequency range of the signals is between 5 and 30 Hz with a maximum between 7 and 20 Hz.

Two examples of record sections are presented in Figs. 47 and 48, one is related to an MLR station located in the Spessart and the other to a station placed in the Taunus mountains. Only about $^1/_3$ of all shots in between the two stations is shown. No clear intracrustal reflectors but a strong P_MP – even in the subcritical range – can be observed at the Spessart station in the SE (Fig. 47) whereas the Taunus station (Fig. 48) in the NW shows two strong intracrustal reflectors and a clear beginning of the P_MP wave from the Moho.

Certainly the velocity-depth structure in the northwestern part of the observed profile section, represented by the Taunus station, is quite different from that of the southwestern part. From the near-vertical data, shown in Figs. 20–23, it becomes clear that major lateral heterogeneities are present, especially below the Spessart mountains, which should show up predominantly in the Spessart profile. The migration of reflection points may then result in a smearing and smoothing of the events as is seen in this seismogram section. The Taunus profile, on the other hand, represents more subhorizontal layering, although the Hessian trough provides also lateral inhomogeneities and a large traveltime delay, especially for the shorter distances.

The interpretation of the complete data set can be expected to result in a more detailed picture of crustal velocities in the northwestern part of DEKORP 2-S, which displays one of the most interesting tectonic developments along the whole profile.

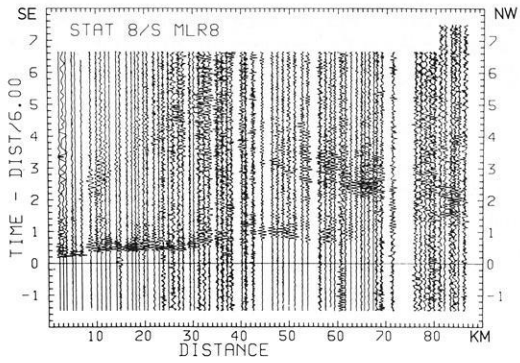

Fig. 47. Reduced record section of a magnetic longtime recording station (MLR) in the Spessart mountains. 4–30 Hz bandpass filter. NW is to the *right*!

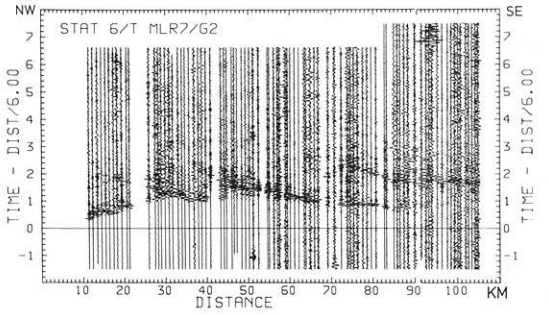

Fig. 48. Reduced record section of a MLR station in the Taunus mountains. Shots between this station and the Spessart station (see Fig. 47) provide a reversed observation scheme. SE is to the right!

5. Conclusions

The DEKORP 2-S profile is the first long range near-vertical reflection profile for crustal studies in Central Europe. Running perpendicular to the Variscan strike it crosses at least two significant geotectonical boundaries and provides many new data. The use of explosives allowed important near-vertical as well as wide-angle experiments yielding valuable additional data sets. The establishment of an independent DEKORP processing center proved to be a major advantage for the handling and interpretation of data.

A major achievement with regard to the tectonic structure along the profile is the confirmation of generally southeast dipping thrust systems. In particular, the boundary between the Saxothuringian and Rhenohercynian zones is marked clearly by strongly dipping reflectors, supposed to represent thrust zones in the upper crust. There are several indications that also the lower crust was involved in the thrust tectonics although this evidence might not be as strong as that of the BIRPS' SWAT profiles or the first Ecors line.

The appearance of several strong diffraction clusters, concentrating in the lower crust, was the greatest surprise of the survey. Although the position of prominent diffractions could be assessed in the case of the Dinkelsbühl clusters by means of a quasi 3-D observation, only speculations

[4] By teams from Bochum, Frankfurt and Munich

can be provided with regard to their origin and nature. The predominantly vertical arrangement of large sets of these diffractions suggests an origin by extensional tectonics, possibly related to the post-Variscan extensional or wrench faulting (Ziegler, 1978; Arthaud and Matte, 1975). This could explain their arrangement along near-vertical planes in the strike direction of the Variscides. On the other hand, the clustering of the diffractions could also be explained by the idea of ramps and huge horses of the large thrust system.

Compared to previously observed crustal reflection profiles in the Variscides (Bartelsen et al., 1982; Meissner et al., 1982, 1983, 1984) the reflectivity pattern is nearly identical. An upper crust, void of reflections except for those of fault zones, is underlain by a dense lamellae-like, highly reflective lower crust. The beginning of this zone at about 4.5–5 s TWT may be related to the Conrad level, their abrupt termination between 9 and 10 s TWT is generally attributed to the Moho. Only very few sporadic reflections are observed from the Upper Mantle. Compared to the Urach profiles a tendency for less correlatable and shorter reflection segments with a dominance of diffraction patterns seems to emerge for the profiles perpendicular to the strike direction, like the DEKORP 2-S line.

One of the major questions not yet answered is the velocity problem. The dominance of diffractions and the shortness and weakness of correlatable reflections made the calculation of reliable stacking velocities extremely difficult. Additional attempts to calculate velocities from the curvature of diffractions, from the various wide-angle experiments and from other processes than the conventional stacking method are well under way and reveal the strong lateral velocity inhomogeneities along and around the main profile. The mapping of exact velocity-depth functions and their application to the tectonic problems of the Variscides is the major challenge for the on-going interpretation.

Such problems are for instance: What does the deep structure of the Northern Phyllite Zone look like? Does it extend beneath the Mid-German Crystalline High? What is the depth extent of the Saxothuringian cover, and what are its structural relations to the basement?

Several groups of scientists in the Federal Republic of Germany are continuing to work on the DEKORP 2-South data, its better processing, analysis and interpretation. Additional ideas will come from the results on other DEKORP-/KTB-profiles surveying the same geological units in analogous tectonic positions. The hope is justified that questions which had to be left open at this time will be answered soon due to these combined geoscientific efforts in the frame of the DEKORP project.

Acknowledgements. The funding of the DEKORP-Project by the Bundesministerium für Forschung und Technologie, Bonn, is gratefully acknowledged. The administrative services are provided by the Niedersächsisches Landesamt für Bodenforschung, Hannover. The excellent performance of the Prakla-Seismos GmbH field crew under the command of Mr. Ceranski has to be emphasized, also the smooth cooperation between all the various groups in the field. Mobil Oil AG, Celle, and Seismograph Service LTD., London, provided the hard- and software, respectively, used at the DEKORP-Processing-Center at Clausthal. Preussag AG and BEB Gewerkschaften Brigitta und Elwerath Betriebsführungsgesellschaft mbH, both in Hannover, supported the work with their modern plotting facilities. The authors thank also the large number of students participating in the field and processing work.

References

Althaus, E., Behr, H.J., Eder, F.W., Goerlich, F., Maronde, D., Ziegler, W.: Kontinentales Tiefbohrprogramm ("KTB") (Continental Deep Drilling Program) of the Federal Republic of Germany. Terra cognita, **4**, 389–397, 1984

Angenheister, G., Pohl, J.: Die seismischen Messungen im Ries 1948–1969. Geol. Bavar., **61**, 304–326, 1969

Angenheister, G., Pohl, J.: Results of seismic investigations in the Ries crater area (Southern Germany). In: Giese, P., Prodehl, C., Stein, A., eds.: Explosion seismology in Central Europe, data and results. Springer, Berlin Heidelberg New York, 1976

Arthaud, F., Matte, Ph.: Le décrochement tardi-hercynienne du sud-ouest de l'Europe – Géométrie et essai de reconstitution des conditions de la déformation. Tectonophysics, **25**, 139–171, 1975

Bally, A.W.: Seismic expression of structural styles – A picture and work atlas; Vol. I The layered earth. AAPG Studies in Geology # 15, Tulsa/Oklahoma, 1983

Bartelsen, H., Lueschen, E, Krey, Th., Meissner, R., Schmoll, J., Walter, Ch.: The Combined Seismic Reflection-Refraction Investigation of the Urach Geothermal Anomaly. In: Haenel, R. (ed.): The Urach Geothermal Project (Swabian Alb – Germany). E. Schweizerbart'sche Verlagsbuchhandlung (Nägele u. Obermiller), Stuttgart, 1982

Behr, H.-J.: Subfluenzprozesse im Grundgebirgsstockwerk Mitteleuropas. Z. Dtsch. geol. Ges., **129**, 291–326, 1978

Behr, H.-J.: Intracrustal and subcrustal thrust-tectonics at the northern margin of the Bohemian Massif. In: Martin, H., Eder, F.W., eds.: Intracontinental fold belts. Springer, Berlin Heidelberg New York Tokyo, 1983

Behr, H.-J., Engel, W., Franke, W., Giese, P., Weger, K.: The Variscan belt in Central Europe: main structures, geodynamic implications, open questions. In: Zwart, H.J., Behr, H.-J., Oliver, J.E., eds.: Appalachian and Hercynian fold belts. Tectonophysics, **109**, 15–50, 1984

Berckhemer, H.: Mars 66: Eine Magnetbandapparatur für seismische Tiefensondierung. Z. Geophys., **36**, 501–518, 1970

Carlé, W.: Bau und Entwicklung der süddeutschen Großscholle. Beih. Geol. Jahrb., **16**, 272 pp., 1955

Carlé, W., Wurm, F.: Die wissenschaftlichen Ergebnisse der Tiefbohrung Allmersbach/Weinberg, Landkreis Backnang, Baden-Württemberg. Jahrb. Geol. Landesamt Baden-Württemberg, **13**, 171–221, 1971

Dohr, G.: Zur reflexionsseismischen Erfassung sehr tiefer Unstetigkeitsflächen. Erdöl Kohle, **10, 5**, 278–281, 1957a

Dohr, G.: Ein Beitrag der Reflexionsseismik zur Erforschung des tieferen Untergrundes. Geol Rundsch., **46**, 17–26, 1957b

Dohr, G, Meißner, R.: Deep Crustal Reflections in Europe. Geophysics, **40**, 25–39, 1975

Eberle, D.: Aeromagnetische Karte der Bundesrepublik Deutschland 1:1.000.00. Hannover: Bundesanstalt für Bodenforschung, 1973

Falke: Zur Paläographie des kontinentalen Perm in Süddeutschland. Abh. Hess. L.-A. Bodenforsch., **60**, 223–234, Wiesbaden: 1971

Gajewski, D., Prodehl, C.: Crustal structure beneath the Swabian Jura, SW Germany, from seismic refraction investigations. J. Geophys., **56**, 69–80, 1985

Gerke, K.: Die Karte der Bouguer-Isanomalen 1:1.000.000 von Westdeutschland. Frankfurt/Main: Institut für Angewandte Geodäsie, 1957

Giese, P.: Die Europäische Geotraverse (EGT). Geowissenschaften: DFG, Dt. Forschungsgemeinschaft, Verlag Chemie, Weinheim, 1983

Giese, P., Prodehl, C., Stein, A., eds.: Explosion seismology in Central Europe, data and results. Springer, Berlin Heidelberg New York, 1976

Golwer, A.: Paläogeographie des Hanauer Beckens im Oligozän und Miozän. Notizbl. Hess. Landesamtes Bodenforsch. Wiesbaden, **96**, 157–184, 1968

Karte der Anomalien der Totalintensität des erdmagnetischen Feldes in der Bundesrepublik Deutschland 1:500.000. Hannover: Bundesanstalt für Geowissenschaften und Rohstoffe, 1976

Kossmat, F.: Gliederung des variszischen Gebirgsbaues. Abh. Sächs. Geol. Landesamt, **1**, 39 pp, 1927

Martin, H., Eder, F.W., eds.: Intracontinental fold belts. Springer, Berlin Heidelberg New York Tokyo, 1983

Masonne, H.J., Schreyer, W.: A new experimental phengite barometer and its application to a Variscan subduction zone at the southern margin of the Rhenohercynicum. Terra cognita, **3**, 187, 1983

Matthes, S.: Die Paragneise im mittleren kristallinen Vorspessart und ihre Metamorphose. Abh. Hess. Landesamt Bodenforsch., **8**, 1–86, 1954

Meissner, R., Bartelsen, H., Murawski, H.: Thin-skinned tectonics in the Northern Rhenish Massif – Germany. Nature, **290**, 399–401, 1981

Meissner, R., Bartelsen, H., Krey, T., Schmoll, J.: Detecting velocity anomalies in the region of the Urach geothermal anomaly by means of new seismic field arrangements. In: Cermak, V., Haenel, R., eds.: Geothermics and geothermal energy. 285–292, Stuttgart, E. Schweizerbart'sche Verlagsbuchhandlung, 1982

Meissner, R., Springer, M., Murawski, H., Bartelsen, H., Flueh, E.R., Duerschner, H.: Combined seismic reflection-refraction investigations in the Rhenish Shield and their relation to recent tectonic movements. In: Fuchs, K., Murawski, H., eds.: Plateau uplift. 276–287. Springer, Berlin Heidelberg New York, 1983

Meissner, R., Springer, M., Flueh, E.: Tectonics of the Variscides in North-Western Germany based on seismic reflection measurements. In: Hutton, D.H.W., Sanderson, D.J., eds.: Variscan Tectonics of the North Atlantic region. Blackwell, 1984

Mostaanpour, M.M.: Einheitliche Auswertung krustenseismischer Daten in Westeuropa – Darstellung von Krustenparametern und Laufzeitanomalien. Berliner Geowiss. Abh., Reihe B, Heft 10, Dietrich Reimer, Berlin, 1984

Trusheim, F.: Über den Untergrund Frankens – Ergebnisse von Tiefbohrungen in Franken und Nachbargebieten 1953–1960. Geol. Bavar., **54**, 1964

Weber, K.: Variscan events – Early palaeozoic continental rift metamorphism and late palaeozoic crustal shortening. In: Hutton, D.H.W., Sanderson, D.J., eds.: Variscan tectonics of the North Atlantic region. Geol. Soc., Spec. Publ., London: 1984

Weber, K., Behr, H.-J.: Geodynamic Interpretation of the Mid-European Variscides. In: Martin, H., Eder, F.W., eds.: Intracontinental fold belts. Springer, Berlin Heidelberg New York Tokyo, 1983

Wenz, W.: Erläuterungen zur geologischen Karte von Hessen – Blatt Rodheim Nr. 5718. 61 pp, Darmstadt: 1936

Ziegler, P.A.: North West Europe Tectonics and Basin Development. Geol. Mijnbouw, **57**, 589–626, 1978

Ziegler, P.A.: Geological Atlas of Western and Central Europe. Elsevier, Amsterdam, 1982

Received June 20, 1985; revised version August 1, 1985
Accepted August 12, 1985